

Dissertation

Biotransformations from and to methylated flavonoids

Subtitle

Benjamin Weigel
Leibniz-Institute of Plant Biochemistry
Department of Bioorganic Chemistry
Weinberg 3
06120 Halle(Saale)
July 13, 2015

Advisor: Prof. Dr. Ludger A. Wessjohann
wessjohann@ipb-halle.de
+49 (345) 5582-1301

noch nicht bekannt

1 **Contents**

2 Notes of Revisors	x
<hr/>	
3 I Preface	1
4 <hr/>	
5 1 Abstracts	2
6 1.1 English Abstract	2
7 1.2 Deutsche Zusammenfassung	2
<hr/>	
8 II Thesis	3
9 <hr/>	
10 2 Introduction	4
11 2.1 Natural products and secondary metabolites	4
12 2.1.1 General	4
13 2.1.2 Classes of natural products	4
14 2.2 Alkylating reactions in nature	5
15 2.2.1 Methylation	5
16 2.2.2 Prenylation	5
17 2.2.3 Glycosylation	5
18 2.3 Usage and expansion of natures reaction toolbox	5
19 2.3.1 Terpene synthases and elongases	5
20 2.3.2 Methyl transferases	5
21 2.3.3 Glycosyl transferases	5
22 2.3.4 Other important enzymes in biotech research	5
23 2.4 Conclusion	5

1	3 Material And Methods	6
2	3.1 Materials	6
3	3.1.1 Chemicals	6
4	3.1.2 Commonly used solutions and buffers	6
5	3.1.3 Culture media used to grow bacteria	8
6	3.1.4 Bacterial strains	8
7	3.1.5 Plasmids	9
8	3.1.6 Oligonucleotides and synthetic genes	10
9	3.1.7 Instruments	10
10	3.1.8 Software	11
11	3.2 Molecular Biology	12
12	3.2.1 Golden Gate Cloning	12
13	3.2.2 Subcloning of genes	13
14	3.2.3 Transformation of electrocompetent <i>Agrobacterium tumefaciens</i> cells	13
15	3.3 Treatment of plant material	13
16	3.3.1 Infiltration of <i>Nicotiana benthamiana</i>	13
17	3.3.2 Plant material harvest	14
18	3.3.3 Extraction of flavonoids from <i>N. benthamiana</i> leaves	14
19	3.4 Protein biochemistry	14
20	3.4.1 Determination of protein concentration	14
21	3.4.2 Protein production test (expression test)	15
22	3.4.3 Protein subfractionation	16
23	3.4.4 Protein sample concentration by TCA precipitation	16
24	3.4.5 Preparation of periplasmic protein	17
25	3.4.6 Discontinuous SDS-polyacrylamide gel electrophoresis (SDS-PAGE)	17
26	3.4.7 Buffer change of protein samples	18
27	3.4.8 Production of recombinant protein	18
28	3.4.9 Preparation of inclusion bodies (IBs)	19
29	3.4.10 Purification of His-tagged proteins using immobilized metal affinity chromatography (IMAC)	20
30	3.4.11 Refolding of SOMT-2 on a micro scale using design of experiments (DoE)	21
31	3.4.12 Enzymatic production of SAM and SAE	23
32	3.5 Crystallographic Procedures	24
33	3.5.1 Crystallization of proteins	24
34	3.5.2 Data collection and processing	25
35	3.5.3 Structure solution	26
36	3.5.4 Model building, refinement and validation	26

1	3.5.5 <i>In silico</i> substrate docking	27
2	3.6 Analytics	27
3	3.6.1 Recording of growth curves	27
4	3.6.2 <i>In vitro</i> determination of glucose	28
5	3.6.3 <i>In vitro</i> O-methyl transferase (O-MT) assay	28
6	3.6.4 Photospectrometric assay for the methylation of catecholic moi- ties.	31
7	3.6.5 Concentration of SOMT-2 using hydrophobic interaction chro- matography (HIC)	32
8	3.6.6 Analytical gel filtration.	32
9	3.6.7 Binding experiments using Isothermal Titration Calorimetry (ITC)	32
10	3.6.8 High-performance liquid chromatography (HPLC) analytics .	33
11	3.6.9 liquid chromatography coupled mass-spectrometry (LC/MS) measurements	33
12	4 Evaluation of PFOMT towards the acceptance of long-chain SAM analogues	34
13	4.1 Introduction	34
14	4.2 <i>In silico</i> docking studies using computational tools	38
15	4.3 Substrate binding studies using ITC.	38
16	4.4 Study of variants for long-chain alkylations	41
17	4.5 Crystallization of PFOMT	42
18	4.6 Conclusion/Discussion	44
19	5 Enzymatic methylation of Non-catechols	49
20	5.1 Introduction	49
21	5.2 SOMT-2.	49
22	5.2.1 In vivo methylation studies using <i>N. benthamiana</i>	49
23	5.2.2 In vivo studies in <i>E. coli</i>	49
24	5.2.3 In vitro studies using recombinantly produced SOMT-2	49
25	5.3 PFOMT	49
26	5.3.1 Acidity and Nucleophilicity of phenolic hydroxyl-groups . . .	49
27	5.3.2 pH-Profiles of PFOMT-catalysis.	49
28	5.3.3 Influence of Mg ²⁺ on PFOMT activity	49
29	5.4 Consensus or Bioinformatic points-of-view (COMT)???	49
30	5.5 Conclusion/Discussion	50
31	6 Development of an whole cell methyl transferase screening sys- tem	51
32	6.1 Introduction	51

1	6.2 Theoretical considerations / design of system	51
2	6.3 Detectability of S-adenosyl-L-homocysteine (SAH)	51
3	6.4 Usage of the lsr-promoter for true autoinduction	51
4	6.5 Conclusion/Discussion	51
5	7 DES in protein crystallography	52
6	7.1 Introduction	52
7	7.2 Solubility enhancement of hydrophobic substances by addition of 8 DES	52
9	7.3 Enzymatic O-methylation in DES	52
10	7.4 DES as precipitants in protein crystallization	52
11	7.5 Conclusion/Discussion	52
12	8 Acknowledgements	53
13	III Appendix	54
14	—	—
15	A Figures	55
16	B Tables	56
17	C Affidavit	61
1	Acronyms	73

List of Figures

3	3.1 Oxidation of the reporter substrate <i>o</i> -dianisidine. Consecutive	
4	one-electron transfers lead to the fully oxidized diimine form of	
5	<i>o</i> -dianisidine. The first electron transfer is believed to produce a charge	
6	transfer complex intermediate. [49, 17]	29
7	3.2 Calibration curves of different relative compositions of ferulic acid to	
8	cafeic acid, that were taken as described in 3.6.4. The total concentra-	
9	tion was always 0.4 mM. At lower pH values around 4, the method	
10	seems to overestimate the concentration of caffeic acid. However, the	
11	slope of the curves stays the same.	31
12	4.1 Graphical representation of the work that has been done on MTs in	
13	combination with SAM analogues. The grey areas represent individual	
14	groups of SAM analogues (aliphatic, allylic, propargylic, aromatic,	
15	SeAM analogues, nitrogen analogues and miscelaneous others). The	
16	height of the grey areas represents the number of times a member of the	
17	corresponding group has been described as tested in the MT literature.	
18	The height of the colored bars represents the times that individual	
19	substrate has been tested. The colors represent the different types of	
20	MT (red – DNA MT, green – P-MT, lilac – small molecule MT, blue –	
21	rna MT). The black dash across the bar shows the number of times this	
22	substrate was actually converted by either enzyme.	36
23	4.2 Labelling of macromolecules by using a combination of novel alkine-	
24	derivatized SAM analogues and Cu ^I -catalyzed azide-alkyne 1,3-dipolar	
25	cycloaddition (CuAAC). Depending on the type of label used, it can be	
26	employed for detection (e.g. through fluorophores, coupled assays) or	
27	affinity purification (e.g. biotin). This technique is also feasable for use	
1	in activity based protein profiling (ABPP) approaches.	37

2 4.3 The binding of different SAM analogues was measured via ITC, but	38
3 also calculated using molecular modelling techniques.	
4 4.4 Exemplary ITC measurements. a – Binding of SAH, SAM and SAE	
5 to PFOMT. b – SAH is injected into a PFOMT solution, with (red) or	
6 without (black) addition of Mg ²⁺ and caffeic acid. When Mg ²⁺ and	
7 caffeic acid were already present, the binding process seems to happen	
8 quicker, but is less enthalpic. c – Upon addition of caffeic acid to the	
9 protein heat is produced, however no sensible binding curve could be	
10 obtained.	40
11 4.5 The active site of PFOMT. The outline of the protein backbone is dis-	
12 played, with active site residues portrayed as colored sticks (cyan –	
13 F103, red – F80, turquoise – M52, yellow – Y51, white – F198, blue	
14 – W184, orange – N202, grey – as labelled). The co-substrate SAM	
15 (ball-and-stick model) was docked into the structure.	42
16 4.6 Some crystal and pseudo-crystal shapes that were observed during the	
17 crytsallization screen. a – high (NH ₄) ₂ SO ₄ , b-c – CaCl ₂ , PEG-4000, e –	
18 LiCl, PEG-6000	43
19 4.7 An overview of the features in the <i>apo</i> -PFOMT structure.	45
20 4.8 Positional differences between the individual residues of the solved <i>apo</i> -	
21 PFOMT and the structure with bound SAH (pdb: 3C3Y). The diffraction	
22 precision indicator [21] (DPI) of the structures was (0.137 and 0.064) Å	
23 respectively. The overall rmsd amounted to 0.9034 Å. The secondary	
24 structure of apo-PFOMT is displayed at the top. Helices are displayed	
25 as rectangles and sheets are shown as arrows. Graphical background	
26 annotations are used to display the binding sites of SAH (green) and	
27 the metal ion (plum). The orange bars indicate regions, where much	
28 movement seems to happen upon binding or release of the co-substrate.	
29 The blue bar shows the region that was annotated as "insertion loop"	
30 in previous studies [57].	46
31 4.9 Comparison of the active sites of the <i>apo</i> -structure (left, green) and	
32 the ligand-bound structure (right, steelblue). Waters are represented	
33 as small red spheres, calcium as a green sphere (complexing bonds	
34 are dashed) and SAH is displayed as a white ball-and-stick model. A	
35 possible hydrogen bond network (blue lines) for the ligand-bound state	
1 is displayed.	47

- 2 4.10 from: Kopycki, J. G., Rauh, D., Chumanovich, A. a., Neumann,
3 P., Vogt, T., & Stubbs, M. T. (2008). Biochemical and Structural
4 Analysis of Substrate Promiscuity in Plant Mg²⁺-Dependent O-
5 Methyltransferases. Journal of Molecular Biology, 378(1), 154–164.
6 http://doi.org/10.1016/j.jmb.2008.02.019 48
- 7 A.1 Differences in the dihedrals ψ (red) and φ (black) of the solved *apo*-
8 PFOMT and the structure with bound SAH (pdb: 3C3Y). The secondary
9 structure is displayed at the top. Helices are displayed as rectangles
10 and sheets are shown as arrows. Graphical background annotations
11 are used to display the binding sites of SAH (green) and the metal ion
12 (plum). The orange bars indicate regions, where much movement seems
13 to happen upon binding or release of the co-substrate. The blue bar
14 shows the region that was annotated as "insertion loop" in previous
1 studies. 55

List of Tables

³ 3.1 NADES-mixtures used within this work.	7
⁴ 3.3 Plasmids used in this work.	9
⁵ 3.4 Primers used in this work. Recognition sites for endonucleases are ⁶ underlined. Positions used for site directed mutagenesis are in lower ⁷ case font.	10
⁸ 3.6 Calculated extinction coefficients of proteins used in this work..	15
⁹ 3.7 Factors used in the construction of the FFD.	21
¹⁰ 3.8 Experimental design matrix for the FFD.	21
¹¹ 4.1 Results of fitting a simple one-site binding model to the data obtained ¹² from ITC experiments.	39
¹³ B.3 SAM analogues that have been used with MTs. Targets: <i>P</i> – pep- ¹⁴ tide/protein, <i>D</i> – DNA, <i>R</i> – RNA, <i>S</i> – small molecule..	56
¹⁵ B.1 Overview over the constructs produced for the present thesis. Each step ¹⁶ during the production of the construct is given in the workflow steps ¹⁷ column. Primers (italic font) or restriction sites used during each step ¹⁸ are displayed in parenthesis.	59
¹ B.4 Crystallographic data, phasing and refinement statistics.	60

² Notes of Revisors

3	BWEIGEL: needs completion	10
4	BWEIGEL: Überprüfen!	19
5	BWEIGEL: ist das korrekt?	25
6	BWEIGEL: To introduction	25
7	BWEIGEL: Lysozym struktur	26
8	BWEIGEL: nochmal auseinanderklamüsern wegen den konzentrationen und eingesetzten enzymmengen...	28
9		
10	BWEIGEL: entweder noch machen oder raus damit	38
11	BWEIGEL: literaturvergleich der umsätze?	41
12	BWEIGEL: LCMS messungen?	41
13	BWEIGEL: Genauer zu den Resten...	41
14	BWEIGEL: grafik?	41
15	BWEIGEL: grafik? & paper	42
16	BWEIGEL: wie groß?	43
17	BWEIGEL: mehr auf die aktuelle literatur eingehen...auch wenn sie sich i grenzen hält...	44
18		
1	BWEIGEL: im buch nochmal bei comt nachlesen	46



2

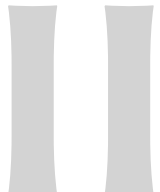
1

Preface

1 Abstracts

1.1 English Abstract

1.2 Deutsche Zusammenfassung



2

1

Thesis

2 Introduction

³ Some introductory text

2.1 Natural products and secondary metabolites

2.1.1 General

2.1.2 Classes of natural products

7 Terpenoids and Steroids

⁸ ... here is some text

9 Polyketides and non-ribosomal peptides

¹⁰ ... here is some text

11 Alkaloids

¹² ... here is some text

13 Phenylpropanoids

¹⁴ ... here is some text Flavonoids and phenyl propanoids have important functions

¹⁵ in nature and can function as protection against high UV-exposure, signaling

¹⁶ molecules or transcriptional regulators [40, 5].

² 2.2 Alkylating reactions in nature

³ **2.2.1 Methylation**

⁴ **2.2.2 Prenylation**

⁵ **2.2.3 Glycosylation**

⁶ 2.3 Usage and expansion of natures reaction tool-box

⁸ **2.3.1 Terpene synthases and elongases**

⁹ **2.3.2 Methyl transferases**

¹⁰ **2.3.3 Glycosyl transferases**

¹¹ **2.3.4 Other important enzymes in biotech research**

¹² **BMVOs**

¹³ **Esterases/Lipases**

¹⁴ **Oxidases**

¹⁵ **Lyases**

¹⁶ **Transaminases**

¹⁷ 2.4 Conclusion

¹ **C**

3 Material And Methods

³ Within this section percentages refer to volume per volume (v/v) percentages unless
⁴ otherwise specified.

3.1 Materials

3.1.1 Chemicals

⁵ Enzymes and buffers used for molecular cloning were obtained from Life Technologies (Darmstadt, Germany), unless otherwise noted. Flavonoid HPLC standards
⁶ were purchased from Extrasynthese (Genay, France). Deuterated solvents were
⁷ acquired from Deutero GmbH (Kastellaun, Germany). Solvents, purchased from
⁸ VWR (Poole, England), were distilled in-house before use.

⁹ All other chemicals were obtained from either Sigma-Aldrich (Steinheim, Ger-
¹⁰ many), Applichem (Darmstadt, Germany), Carl Roth (Karlsruhe, Germany) or
¹¹ Merck (Darmstadt, Germany).

3.1.2 Commonly used solutions and buffers

50× 5052	25 % glycerol, 2.5 % (w/v) glucose, 10 % (w/v) α-lactose
binding buffer	50 mM Tris/HCl, 500 mM NaCl, 10 % glycerol, 2.5 mM imidazole pH 7
elution buffer	50 mM Tris/HCl, 500 mM NaCl, 10 % glycerol, 250 mM imida- zole pH 7

lysis buffer	50 mM Tris/HCl, 500 mM NaCl, 10 % glycerol, 2.5 mM imidazole, 0.2 % Tween-20 pH 7
1 M MMT pH 4 (10×)	26.8 g/l L-malic acid, 78.1 g/l MES, 26.8 g/l Tris, 2.1 % 10 M HCl
1 M MMT pH 9 (10×)	26.8 g/l L-malic acid, 78.1 g/l MES, 26.8 g/l Tris, 6.7 % 10 M NaOH
20× NPS	1 M Na_2HPO_4 , 1 M KH_2PO_4 , 0.5 M $(\text{NH}_4)_2\text{SO}_4$
1 M SSG pH 4 (10×)	14.8 g/l succinic acid, 60.4 g/l $\text{NaH}_2\text{PO}_4 \cdot \text{H}_2\text{O}$, 32.8 g/l glycine, 0.4 % 10 M NaOH
1 M SSG pH 10 (10×)	14.8 g/l succinic acid, 60.4 g/l $\text{NaH}_2\text{PO}_4 \cdot \text{H}_2\text{O}$, 32.8 g/l glycine, 10.3 % 10 M NaOH
5× SDS sample buffer	10 % (w/v) SDS, 10 mM β -mercaptoethanol, 20 % glycerol, 0.2 M Tris/HCl pH 6.8, 0.05 % (w/v) bromophenolblue
1000× trace elements	50 mM FeCl_3 , 20 mM CaCl_2 , 10 mM MnCl_2 , 10 mM ZnSO_4 , 2 mM CoCl_2 , 2 mM CuCl_2 , 2 mM NiCl_2 , 2 mM Na_2MoO_4 , 2 mM Na_2SeO_3 , 2 mM H_3BO_3

Preparation of natural deep eutectic solvent (NADES)

NADES were prepared by adding each component in a round-bottom flask with a stirrer and stirring the mixture at 50 °C with intermittent sonication treatments until a clear solution was obtained.

Table 3.1.: NADES-mixtures used within this work.

name	composition	mole ratio	mass fraction (w/w)
PCH	propane-1,2-diol	1:1:1	0.326
	choline chloride		0.597
	water		0.077
GCH	L-glucose	2:5:5	0.314
	choline chloride		0.608
	water		0.078

² 3.1.3 Culture media used to grow bacteria

LB-medium	10 g/l NaCl, 10 g/l tryptone, 5 g/l yeast extract, pH 7.5
LB-agar	LB + 1.5 % (w/v) agar-agar
TB-medium	12 g/l tryptone, 24 g/l yeast extract, 0.4% glycerol, 72 mM K ₂ HPO ₄ , 17 mM KH ₂ PO ₄
ZY	10 g/l tryptone, 5 g/l yeast extract
ZYP-5052	volume fraction (v/v): 0.928 ZY, 0.05 20× NPS, 0.02 50× 5052, 0.002 1 M MgSO ₄ , 0.0002 1000× trace elements

³ 3.1.4 Bacterial strains

¹ *E.coli*

BL21(DE3)	F ⁻ <i>ompT hsdSB(r_B⁻,m_B⁻) gal dcm λ</i> (DE3) Invitrogen, Karlsruhe (Germany)
C41(DE3)	F ⁻ <i>ompT hsdSB(r_B⁻,m_B⁻) gal dcm λ</i> (DE3) Lucigen, Wisconsin (USA)
C43(DE3)	F ⁻ <i>ompT hsdSB(r_B⁻,m_B⁻) gal dcm λ</i> (DE3) Lucigen, Wisconsin (USA)
DH5α	F ⁻ <i>Φ80lacZΔM15 Δ(lacZYA-argF) U169 recA1 endA1 hsdR17(r_K⁻m_K⁺) phoA supE44 λ⁻ thi-1 gyrA96 relA1</i> Invitrogen, Karlsruhe (Germany)
JM110	<i>rpsL thr leu thi lacY galK galT ara tonA tsx dam dcm glnV44 Δ(lac-proAB) e14- [F' traD36 proAB⁺ lacI^q lacZΔM15] hsdR17(r_K⁻m_K⁺)</i> Martin-Luther-University Halle-Wittenberg
JW1593 (BW25113 derivative)	<i>rrnB ΔlacZ4787 HsdR514 Δ(araBAD)568 rph-1 ΔydgG (Kan^R)</i> Keio Collection, National Institute of Genetics (Japan)
MG1655	F ⁻ <i>λ⁻ ilvG⁻ rfb-50 rph-1</i> DSMZ, Hamburg (Germany)

One Shot TOP10	F ⁻ $\Phi 80lacZ\Delta M15 \Delta(mrr-hsdRMS-mcrBC) recA1 endA1 mcrA \Delta lacX74 araD139 \Delta(ara-leu)7697 galU galK rpsL (\text{Str}^R) \lambda^- nupG$ Invitrogen, Karlsruhe (Germany)
Origami(DE3)	$\Delta(ara-leu)7697 \Delta lacX74 \Delta phoA P_{vfull} phoR araD139 ahpC galE galK rpsL F' [lac + lacI q pro]$ (DE3) <i>gor522::Tn10 trxB</i> (Kan ^R , Str ^R , Tet ^R) Novagen, Wisconsin (USA)
Rosetta(DE3)	F ⁻ <i>ompT hsdSB(r_B⁻,m_B⁻) gal dcm λ(DE3) pRARE (Cam^R)</i> Novagen, Wisconsin (USA)
Rosetta(DE3) pLysS	F ⁻ <i>ompT hsdSB(r_B⁻,m_B⁻) gal dcm λ(DE3) pLysSRARE (Cam^R)</i> Novagen, Wisconsin (USA)
T7 Express	<i>fhuA2 lacZ::T7 gene1 [lon] ompT gal sulA11 R(mcr-73::miniTn10-Tet^S)2 [dcm] R(zgb-210::Tn10-Tet^S) endA1 Δ(mcrC-mrr)114::IS10</i> NEB, Massachusetts (USA)

Agrobacterium tumefaciens

GV3101	chromosomal background: C58, marker gene: <i>rif</i> , Ti-plasmid: cured, opine: nopaline Sylvestre Marillonet, IPB
--------	---

3.1.5 Plasmids**Table 3.3.: Plasmids used in this work.**

name	supplier/source
pACYCDuet-1	Merck, Darmstadt (Germany)
pCDFDuet-1	Merck, Darmstadt (Germany)
pET-20b(+)	Merck, Darmstadt (Germany)
pET-28a(+)	Merck, Darmstadt (Germany)
pET-32a(+)	Merck, Darmstadt (Germany)
pET-41a(+)	Merck, Darmstadt (Germany)

name	supplier/source
pQE30	QIAGEN, Hilden (Germany)
pUC19	Invitrogen, Karlsruhe (Germany)

3.1.6 Oligonucleotides and synthetic genes

Oligonucleotides and primers were ordered from Eurofins Genomics (Ebersberg, Germany). The purity grade was *high purity salt free* (HPSF). Synthetic genes or gene fragments were obtained from GeneArt® (Life Technologies, Darmstadt, Germany) or Eurofins Genomics (Ebersberg, Germany).

BWEIGEL: needs completion

Table 3.4.: Primers used in this work. Recognition sites for endonucleases are underlined. Positions used for site directed mutagenesis are in lower case font.

name	sequence (5'→3')	cloning site
somt1	TTG <u>AAG ACA</u> AAA TGG CTT CTT CAT TAA ACA ATG GCC G	BpiI
somt2	TTG <u>AAG ACA</u> AGG ACA CCC CAA ATA CTG TGA GAT CTT CC	BpiI
somt3	TTG <u>AAG ACA</u> AGT CCT TAG GAA CAC CTT TCT GGG AC	BpiI
somt4	TTG <u>AAG ACA</u> AAA GCT CAA GGA TAG ATC TCA ATA AGA GAC	BpiI
pfomt1/fw	CAG AGA GGC cTA TGA GAT TGG CTT GC	
pfomt1/rv	GCA AGC CAA TCT CAT AgG CCT CTC TG	
pfomt2/fw	<u>CAT ATG</u> GAT TTT GCT GTG ATG AAG CAG GTC	NdeI
pfomt2/rv	<u>GAA TTC</u> AAT AAA GAC GCC TGC AGA AAG TG	EcoRI
pRha1/fw	CTC TAG <u>CAG ATC</u> TCG GTG AGC ATC ACA TCA CCA CAA TTC	BglII
pRha1/rv	CAA TTG <u>AGG ATC</u> CCC ATT TTA ACC TCC TTA GTG	BamHI
pUC1/fw	GCG TAT TGG Gag aTC TTC CGC TTC CTC	
pUC1/rv	GAG GAA GCG GAA GAt ctC CCA ATA CGC	

3.1.7 Instruments

CD-spectrometer	Jasco J-815 (Eaton, USA)
electrophoresis (horizontal)	Biometra Compact XS/S (Göttingen, Germany)
electrophoresis (vertical)	Biometra Compact M (Göttingen, Germany) Biometra Minigel-Twin (Göttingen, Germany)
FPLC	AKTA purifier (GE Healthcare, Freiburg, Germany)
GC/MS	GC-MS-QP2010 Ultra (Shimadzu, Duisburg, Germany)
HPLC	VWR-Hitachi LaChrom Elite (VWR, Darmstadt, Germany)
ITC	MicroCal iTC200 (Malvern, Worcestershire, UK)
plate-reader	SpectraMax M5 (Molecular Devices, Biberach, Germany)
NMR-spectrometer	Varian Unity 400 (Agilent, Böblingen, Germany) Varian VNMRS 600 (Agilent, Böblingen, Germany)
photospectrometer	Eppendorf Biophotometer Plus (Hamburg, Germany) JASCO V-560 (Eaton, USA)
centrifuges	Colibri Microvolume Spectrometer (Biozym, Hess. Oldendorf, Germany) Eppendorf 5424 (Hamburg, Germany) Hettich Mikro 120 (Kirchlengern, Germany)
centrifuge rotors	Beckman Avanti J-E, Beckman Allegra X-30R (Krefeld, Germany) Beckman JA-10, JA-16.250, JS-4.3 (Krefeld, Germany)

3.1.8 Software

³ All mathematical and statistical computations and graphics were done with the R software (versions 3.1.X, <http://cran.r-project.org/>) [91]. Visualizations of macro-molecules were arranged using the PyMol Molecular Graphics System, version 1.7.0.0 (Schrödinger, New York, USA).

⁷ Physicochemical calculations and calculations of different molecular descriptors were performed using Marvin Beans 15.4.13.0 (ChemAxon, Budapest, Hungary) and ⁹ Molecular Operating Environment 2008.10 (Chemical Computing Group, Montreal, ¹⁰ Canada). Special software used for X-ray crystal structure solution is discussed ¹ separately in the corresponding section (3.5).

3.2 Molecular Biology

³ Basic molecular biology methods like polymerase chain reaction (PCR), DNA re-
⁴ striction/ligation, DNA gel electrophoresis, preparation of competent cells and
⁵ transformation were performed based on the protocols summarized by Sambrook
⁶ and Russell [99].

⁷ Plasmid DNA was isolated using the QIAprep® Spin Miniprep Kit (QIAGEN, Hilden,
⁸ Germany) according to the manufacturer's instructions.

⁹ In vitro site-directed mutagenesis was set-up according to the protocol of the
¹⁰ QuikChange™ Site-Directed Mutagenesis kit [2] offered by Agilent Technologies
¹¹ (Santa Clara, USA).

¹² Nucleotide fragments obtained by PCR, restriction/ligation procedures or excision
¹³ from electrophoresis gels were purified and concentrated using the *Nucleospin Gel*
¹⁴ and *PCR Clean-up* kit provided by Machery-Nagel (Düren, Germany) according to
¹⁵ the instructions provided by the manufacturer.

3.2.1 Golden Gate Cloning

¹⁷ The Golden Gate cloning procedure is a one-pot method, meaning the restriction
¹⁸ digestion and ligation are carried out in the same reaction vessel at the same time
¹⁹ [56, 30]. Consequently PCR-fragments, destination vector, restriction endonuclease
²⁰ and ligase are added together in this reaction. The methodology employs type II
²¹ restriction enzymes, which together with proper design of the fragments allow for
²² a ligation product lacking the original restriction sites.

²³ For digestion/ligation reactions of fragments containing BpiI sites, 20 fmol of each
²⁴ fragment or vector, together with 5 U of BpiI and 5 U of T4 ligase were combined in
²⁵ a total volume of 15 µl 1× ligase buffer. For fragments to be cloned via BsaI sites,
²⁶ BpiI in the above reaction was substituted by 5 U BsaI.

²⁷ The reaction mixture was placed in a thermocycler and incubated at 37 °C for
²⁸ 2 min and 16 °C for 5 min. These two first steps were repeated 50 times over. Finally,
²⁹ the temperature was raised to 50 °C (5 min) and 80 °C (10 min) to inactivate the
¹ enzymes.

3.2.2 Subcloning of genes

All subcloning procedures were performed according to section 3.2 and specifically subsection 3.2.1. Specific steps for the subcloning of any genes discussed can be found in the appendix (p.59). The *pfomt* gene was subcloned from the pQE-30 vector kindly provided by Thomas Vogt (Leibniz-Institute of Plant Biochemistry (IPB), Halle, Germany) into the pET-28a(+) vector. The *somt-2* gene was subcloned from the pQE-30 vector kindly provided by Martin Dippe (IPB, Halle, Germany) into the pET-28-MC vector.

3.2.3 Transformation of electrocompetent *Agrobacterium tumefaciens* cells

A 50 µl aliquot of electrocompetent *A. tumefaciens* cells was thawed on ice. (50 to 100) ng of plasmid were added, the solution was mixed gently and transferred to a pre-cooled electroporation cuvette. After pulsing (2.5 kV, 200 Ω) 1 ml of lysogeny broth (LB)-medium was added, the mixture transferred to a 1.5 ml tube and incubated for (3 to 4) hours at 28 °C. The culture was centrifuged (10 000 × g, 1 min) and 900 µl supernatant were discarded. The pellet was resuspended in the remaining liquid, plated onto LB-agar plates supplemented with 40 µg/ml rifampicin and 50 µg/ml carbencillin and incubated at 28 °C for (2 to 3) days.

3.3 Treatment of plant material

3.3.1 Infiltration of *Nicotiana benthamiana*

Before infiltration *N. benthamiana* plants were pruned, such that only leaves to be infiltrated remained with the plant. 5 ml cultures of transformed *A. tumefaciens* in LB-medium (with 40 µg/ml rifampicin and 50 µg/ml carbencillin) were grown over night at 28 °C and 220 rpm. OD⁶⁰⁰ of the culture was measured and adjusted to 0.2 by dilution with infiltration buffer (10 mM MES/NaOH, 10 mM MgSO₄ pH 5.5). When multiple *A. tumefaciens* transformed with different constructs/plasmids were used for infiltration, the cultures were mixed and diluted using infiltration buffer,

such that OD⁶⁰⁰ of each culture in the mix was 0.2. The solution was infiltrated into the abaxial side of *N. benthamiana* leaves using a plastic syringe. The leaf material was harvested after 7 days.

3.3.2 Plant material harvest

Infiltrated/Infected areas of *N. benthamiana* leaf material were cut out and grouped by plant number, leaf position (top/bottom) and leaf side (right/left). The grouped clippings were weighed, frozen in liquid nitrogen, ground to a powder, freeze-dried and stored at -80 °C.

3.3.3 Extraction of flavonoids from *N. benthamiana* leaves

Two tips of a small spatula of freeze-dried material (\approx 6 mg), were weighed exactly and extracted with 500 µl 75 % aqueous methanol containing 1 mM ascorbic acid, 0.2 % formic acid and 0.1 mM flavone (internal standard). Therefore the suspension was vortexed for 30 s, rotated on an orbital shaker for 10 min and vortexed again for 30 s. The suspension was centrifuged (20 000 $\times g$, 4 °C, 10 min) and the supernatant transferred to a new tube, to remove the insoluble plant material. The supernatant was centrifuged again (20 000 $\times g$, 4 °C, 10 min) and the resulting supernatant was transferred to a HPLC-vial and stored at -20 °C until analysis.

3.4 Protein biochemistry

Stock solutions of antibiotics, IPTG or sugars were prepared according to the pET System Manual by Novagen [86], unless otherwise noted.

3.4.1 Determination of protein concentration

Protein concentrations were estimated using the absorption of protein solutions at 280 nm, which is mainly dependent on the amino acid composition of the protein studied [37]. Extinction coefficients of proteins were calculated from the amino acid sequence using the ExpPASy servers's ProtParam tool [36].

Table 3.6: Calculated extinction coefficients of proteins used in this work.

protein/enzyme	$\epsilon_{280\text{nm}}^{1\text{g/l}}$ in $\text{ml mg}^{-1} \text{cm}^{-1}$
PFOMT (reduced)	0.714
PFOMT Y51K N202W (reduced)	0.852
SOMT-2 (oxidized)	1.263
SOMT-2 (reduced)	1.247
COMT	

3.4.2 Protein production test (expression test)

³ The heterologous production of proteins in *E. coli* was assessed in a small scale
⁴ protein production test, henceforth called expression test. Single colonies of *E. coli*
⁵ transformed with the constructs to be studied were used to inoculate a 2 ml starter
⁶ culture in LB-medium containing the appropriate antibiotics. The working con-
⁷ centrations of antibiotics used was as follows: 200 µg/ml ampicillin, 150 µg/ml
⁸ kanamycin, 50 µg/ml chloramphenicol, 20 µg/ml tetracycline.

⁹ The starter culture was allowed to grow at 37 °C and 200 rpm over night. A 5 ml
¹⁰ sampling culture of the medium to be studied containing the appropriate antibiotics
¹¹ was prepared. The media tested included LB, terrific broth (TB) and auto-induction
¹² media like ZYP-5052. The sampling culture was inoculated to an OD⁶⁰⁰ of 0.075
¹³ using the starter culture and incubated at different temperatures and 200 rpm in a
¹⁴ shaking incubator. 1 mM isopropyl-D-thiogalactopyranosid (IPTG) was added when
¹⁵ the OD⁶⁰⁰ reached 0.6-0.8, if appropriate for the studied construct. 1 ml samples
¹⁶ were removed after different times of incubation (e.g. 4, 8, 12 hours), subfraction-
¹⁷ ated (3.4.3) and analyzed via SDS-polyacrylamide gel electrophoresis (PAGE) (3.4.6).
¹⁸ Exact specifications of growth conditions (e.g. temperature, time, constructs) are
¹⁹ discussed in the individual sections.

3.4.3 Protein subfractionation

The protein subfractionation procedure described herein was adapted from the protocol described in the pET Manual [86]. Overall 5 protein subfractions can be obtained, including *total cell protein*, *culture supernatant (medium) protein*, *periplasmic protein*, *solute cytoplasmic protein* and *insoluble protein*.

The OD⁶⁰⁰ of the culture sample was measured and the cells harvested by centrifugation at 10 000 × g, 4 °C for 5 minutes. The protein in the supernatant medium was concentrated by precipitation with trichloro acetic acid (TCA) (3.4.4) for SDS-PAGE analysis. The periplasmic protein was prepared (3.4.5) and also concentrated by TCA precipitation for SDS-PAGE. Cells were lysed by resuspending the cell pellet in (OD⁶⁰⁰ × V × 50) µl of bacterial protein extraction reagent (B-PER) and vortexing vigorously for 30 s. The suspension was incubated at room temperature (RT) for 30 min to assure complete lysis. To separate insoluble protein and cell debris from the soluble cytosolic protein, the suspension was centrifuged at 10 000 × g and 4 °C for 10 min. Soluble cytoplasmic protein was contained in the supernatant, whereas insoluble protein remained in the pellet. For SDS-PAGE analysis of the insoluble protein, the pellet was resuspended in the same volume of B-PER. To obtain only the total cell protein fraction, the preparation of periplasmic and soluble cytosolic protein was omitted. Sample volumes of 10 µl of each fraction were used for SDS-PAGE analysis.

3.4.4 Protein sample concentration by TCA precipitation

Diluted protein samples were concentrated by TCA precipitation in microcentrifuge tubes. Therefore 0.1 volume (V) of 100 % (w/v) TCA in water was added to the clarified sample, which was then vortexed for 15 s and placed on ice for a minimum of 15 min. The sample was centrifuged at 14 000 × g, 4 °C for 15 min. The supernatant was discarded and the pellet was washed twice with 0.2 V ice-cold acetone. The acetone was removed and the pellet set to air-dry in an open tube. After drying, the protein pellet was resuspended in 0.1 V phosphate buffered saline (PBS) containing 1 × SDS-sample buffer by heating to 85 °C and vigorous vortexing, to achieve a

² 10 × concentration. After resuspension the sample was analyzed by SDS-PAGE or
³ stored at -20 °C until use.

⁴ 3.4.5 Preparation of periplasmic protein

⁵ Target proteins may be directed to the periplasmic space by N-terminal signal
⁶ sequences like *pelB* or *DsbA/C* [74]. The periplasma is, other than the cytosol, an
⁷ oxidizing environment and often used for the production of proteins containing
⁸ disulfide linkages. The preparation of periplasmic protein was accomplished by an
⁹ osmotic shock protocol modified from Current Protocols in Molecular Biology [7].
¹⁰ The cell pellet was resuspended in the same volume as the culture sample of 30 mM
¹¹ tris-HCl, 20 % (w/v) sucrose, pH 8 and 1 mM ethylenediaminetetraacetic acid (EDTA)
¹² was added. The suspension was stirred for 10 min at RT and the cells were collected
¹³ by centrifugation at 10 000 × g, 4 °C for 10 min. The supernatant was discarded
¹⁴ and the cell pellet was resuspended in the same volume of ice-cold 5 mM MgSO₄.
¹⁵ The suspension was stirred for 10 min on ice, while the periplasmic proteins were
¹⁶ released into the solution. The cells were collected by centrifugation as before.
¹⁷ Periplasmic proteins were contained in the supernatant.

¹⁸ 3.4.6 Discontinuous SDS-polyacrylamide gel electrophoresis ¹⁹ (SDS-PAGE)

²⁰ The analysis of samples via SDS-PAGE was realized via the discontinuous system
²¹ first described by Laemmli, which allows separation of proteins based on their
²² electrophoretic mobility, which in turn depends on their size [59].

²³ The SDS-PAGE procedure was carried out according to standard protocols described
²⁴ by Sambrook and Russell [99]. Very dilute and/or samples with high ionic strength
²⁵ were concentrated and/or desalting by the TCA precipitation procedure described in
²⁶ subsection 3.4.4. Generally a 10 % (acrylamide/bisacrylamide) running gel combined
²⁷ with a 4 % stacking gel was used. Reducing SDS-PAGE sample buffer was added to
²⁸ the protein sample to be analyzed, whereafter the sample was heated to 95 °C for
²⁹ 5 min, to allow for total unfolding of the protein. After cooling to RT the samples
¹ were transferred into the gel pockets for analysis. The *PageRuler™ Prestained*

² Protein Ladder (Life Technologies GmbH, Darmstadt, Germany) was used as a
³ molecular weight (MW) marker and run alongside every analysis as a reference.
⁴ Gels were stained using a staining solution of 0.25 % Coomassie Brilliant Blue G-
⁵ 250 (w/v) in water:methanol:acetic acid (4:5:1) and destained by treatment with
⁶ water:methanol:acetic acid (6:3:1).

⁷ 3.4.7 Buffer change of protein samples

⁸ The buffer in protein samples was exchanged either by dialysis, or by centrifugal
⁹ filter concentrators (Amicon® Ultra Centrifugal Filter; Merck, Darmstadt, Ger-
¹⁰ many). Large volumes of highly concentrated protein solutions were preferably
¹¹ dialyzed. Respectively, very dilute samples were concentrated and rebuffed using
¹² centrifugal concentrators.

¹³ Dialysis was carried out at least twice against a minimum of 100 times the sample
¹⁴ volume. Dialysis steps were carried out at RT for 2 hours, or over-night at 4 °C.
¹⁵ Centrifugal concentrators were used according to the manufacturers instructions.

¹⁶ 3.4.8 Production of recombinant protein

¹⁷ Heterologous production of PFOMT

¹⁸ PFOMT was produced as a N-terminally (His)₆-tagged fusion protein. A 2 ml starter
¹⁹ culture of LB containing 100 µg/ml kanamycin was inoculated with a single colony
²⁰ of *E. coli* BL21(DE3) transformed with pET28-pfomt and incubated at 37 °C, 220 rpm
²¹ for 6 hours. The main culture (N-Z-amino, yeast extract, phosphate (ZYP-5052)
²² containing 200 µg/ml kanamycin) was inoculated with the starter culture such that
²³ OD⁶⁰⁰ was 0.05. The culture was incubated in a shaking incubator at 37 °C, 220 rpm
²⁴ over night (~16 h). Due to the autoinducing nature of the ZYP-5052 medium, addi-
²⁵ tion of IPTG was not necessary. Cells were harvested by centrifugation at 10 000 × g,
²⁶ 4 °C for 10 min and the supernatant discarded. The pellet was resuspended in 50 mM
²⁷ Tris/HCl, 500 mM NaCl, 2.5 mM imidazole, 10 % glycerol pH 7 using a volume of
²⁸ ~10 ml/g of cell pellet. The cells were lysed by sonication (70 % amplitude, 1 s on-
off-cycle) for 30 seconds, which was repeated twice. The crude lysate was clarified

2 by centrifugation at $15\,000 \times g$, 4 °C for 15 minutes followed by filtration through a
3 0.45 µm filter. Consequently, the His-tagged PFOMT was purified by immobilized
4 metal affinity chromatography (IMAC) (3.4.10). The eluted PFOMT protein was
5 dialyzed (3.4.7) against 25 mM HEPES, 100 mM NaCl, 5 % glycerol pH 7 and stored
6 at -20 °C until use.

7 **Heterologous production of SOMT-2**

8 SOMT-2 was produced as a fusion protein with an N-terminal His-tag. A starter
9 LB-culture (≈ 2 ml) containing 100 µg/ml kanamycin was inoculated with a single
10 colony of *E. coli* BL21(DE3) transformed with pET28MC-somt and incubated at BWEIGEL: Überprüfen!
11 37 °C, 220 rpm for 6 hours. The starter culture was used to inoculate the main
12 culture (LB-medium containing 100 µg/ml kanamycin), such that $OD^{600} \approx 0.05$.
13 The culture was incubated at 37 °C, 220 rpm in a shaking incubator until OD^{600}
14 ≈ 0.6 . Expression was induced by addition of 1 mM IPTG. Incubation continued at
15 37 °C, 220 rpm for 6 hours. Cells were harvested by centrifugation ($10\,000 \times g$, 4 °C,
16 10 min) and used, or stored at -20 °C until use. SOMT-2 was produced in inclusion
17 bodies (IBs), which were prepared as laid out in subsection 3.4.9.

18 **3.4.9 Preparation of inclusion bodies (IBs)**

19 Often, when recombinant protein is produced in high levels in *E. coli* it is accumu-
20 lated in so-called inclusion bodies (IBs) [96]. The accumulating IBs consist mainly
21 of the overproduced target protein, which is inherently quite pure already. IBs can
22 be selectively recovered from *E. coli* cell lysates and can consequently be refolded.
23 IBs were prepared according to a modified protocol by Palmer [88].

24 The cells were resuspended in 5 ml/g_{cells} IB lysis buffer (100 mM Tris/HCl, 1 mM
25 EDTA pH 7), 0.5 mM phenylmethylsulfonylfluoride (PMSF) was added as protease
26 inhibitor. The solution was homogenized using a tissue grinder homogenizer (Ultra
27 Turrax®; IKA®-Werke GmbH & Co. KG, Staufen, Germany). 200 µg/ml lysozyme
28 was added to aid in the breakage of cells and the cells were lysed by sonicating
29 thrice at 70 % amplitude (1 s on-off-cycle) for 30 seconds. DNase I (10 µg/ml) was
1 added and the solution was incubated on ice for 10 min. The lysate was clarified by

2 centrifuging for 1 h at 20 000 × *g*, 4 °C. The supernatant was discarded and the pellet
3 was resuspended in 5 ml/g_{cells} IB wash buffer I (20 mM EDTA, 500 mM NaCl, 2 %
4 (w/v) Triton X-100 pH), followed by thorough homogenization. The solution was
5 centrifuged (30 min at 20 000 × *g*, 4 °C), the supernatant discarded and the pellet
6 was washed twice more. To remove detergent, the pellet was washed twice again
7 with IB washing buffer II (20 mM EDTA, 100 mM Tris/HCl pH 7). The IBs were
8 resuspended in IB solubilization buffer (100 mM Tris/HCl, 5 mM DTT, 6 M GdmCl
9 pH 7), such that the protein concentration was about 25 mg/ml and stored at -20 °C
10 until use.

11 3.4.10 Purification of His-tagged proteins using immobilized 12 metal affinity chromatography (IMAC)

13 N- or C-terminal oligo-histidine tags (His-tags) are a common tool to ease purification
14 of recombinantly produced proteins. The free electron pairs of the imidazol
15 nitrogens of histidines can complex divalent cations such as Mg²⁺ or Ni²⁺, which
16 are usually immobilized on a matrix of nitrilo triacetic acid (NTA)-derivatives. The
17 affinity of the His-tag is correlated with its length and tagged proteins can simply
18 be eluted by increasing the concentration of competing molecules (e.g. imidazole).
19 His-tagged protein was purified by fast protein liquid chromatography (FPLC) via
20 Ni²⁺- (HisTrap FF crude) or Co²⁺-NTA (HiTrap Talon FF crude) columns, obtained
21 from GE Healthcare (Freiburg, Germany), following modified suppliers instructions.
22 First the column was equilibrated with 5 column volumes (CV) of binding buffer
23 (50 mM Tris/HCl, 500 mM NaCl, 10 % glycerol, 2.5 mM imidazole pH 7). The sample
24 (generally clarified lysate) was applied to the column using a flow of 0.75 ml/min.
25 Unbound protein was removed by washing with 3 CV binding buffer. Unspecifically
26 bound proteins were washed away by increasing the amount of elution buffer
27 (50 mM Tris/HCl, 500 mM NaCl, 10 % glycerol, 250 mM imidazole pH 7) to 10 %
28 (constant for 3 to 5 CV). Highly enriched and purified target protein was eluted
1 with 6 to 10 CV of 100 % elution buffer.

3.4.11 Refolding of SOMT-2 on a micro scale using design of experiments (DoE)

Design of experiments (DoE) and FFD have been successfully used to optimize the refolding conditions of several proteins [122, 3, 8]. Thus, an approach using FFD was used to find optimal refolding conditions for SOMT-2.

Factors studied were pH (buffer), arginine, glycerol, divalent cations, ionic strength, redox system, cyclodextrin and co-factor addition. The experimental matrix was constructed using the FrF2 package (<http://cran.r-project.org/web/packages/FrF2/index.html>) in the R software.

Table 3.7: Factors used in the construction of the FFD.

factor	symbol	setting		unit
		-1	+1	
pH	A	5.5	9.5	-
arginine	B	0	0.5	M
glycerol	C	0	10	% (v/v)
divalent cations ¹	D	no	yes	-
ionic strength ²	E	low	high	-
redox state ³	F	reducing	redox-shuffling	-
α -cyclodextrin	G	0	30	mM
SAH	H	0	0.5	mM

Table 3.8: Experimental design matrix for the FFD.

Experiment	A	B	C	D	E	F	G	H
1	+	+	+	-	-	-	-	+
2	-	-	-	-	-	-	-	-

¹no: 1 mM EDTA; yes: 2 mM CaCl₂, MgCl₂

²low: 10 mM NaCl, 0.5 mM KCl; high: 250 mM NaCl, 10 mM KCl

³reducing: 5 mM DTT; redox-shuffling: 1 mM glutathione (GSH), 0.2 mM glutathione disulfide (GSSG)

Experiment	A	B	C	D	E	F	G	H
3	+	-	+	+	-	+	+	-
4	-	+	+	-	+	+	+	-
5	+	+	-	-	+	+	-	-
6	-	+	-	+	+	-	+	+
7	+	+	-	+	-	-	+	-
8	-	-	+	-	+	-	+	+
9	+	-	+	+	+	-	-	-
10	-	-	-	-	-	+	+	+
11	+	-	-	+	+	+	-	+
12	-	+	+	+	-	+	-	+

2 The buffers were mixed from stock solutions and prepared in 1.5 ml microcen-
 3 trifuge tubes immediately prior to the experiment. 50 µl of solubilized SOMT-2
 4 (1 mg/ml) in IB solubilization buffer was added to each buffer followed by a short
 5 vortex boost for rapid mixing. The final protein concentration in the refolding
 6 reaction was 50 µg/ml, whereas the remaining GdmCl concentration was ≈286 mM.
 7 The refolding reactions were incubated at RT for 1 hour, followed by an over
 8 night incubation at 4 °C. After incubation the refolding reactions were centrifuged
 9 (10 000 × g, 4 °C, 10 min) to separate insoluble and soluble protein fractions. The
 10 supernatant was transferred to a new tube, whereas the pellet was washed twice
 11 with 200 µl acetone and once with 400 µl methanol/acetone (1:1). The pellet was
 12 resuspended in 100 µl PBS with 20 µl SDS-PAGE sample buffer and 10 µl were used
 13 for SDS-PAGE analysis.

14 100 µl of the supernatant were concentrated using TCA precipitation (3.4.4) and
 15 analyzed by SDS-PAGE. The remaining supernatant was rebuffered into 50 mM
 16 2-[Bis(2-hydroxyethyl)amino]-2-(hydroxymethyl)propane-1,3-diol (BisTris) pH 7.5
 17 using Amicon® Ultra 0.5 ml centrifugal filters (Merck, Darmstadt, Germany)
 18 according to the manufacturers instructions. The pre-weighed collection tubes
 19 were re-weighed after recovery and the volume of recovered liquid calculated
 20 ($\rho \approx 1 \text{ g/cm}^3$). The sample was filled up to 100 µl using 50 mM BisTris pH 7.5 and
 1 the protein concentration was assessed using the Roti®-Quant protein quantifi-

cation solution (Carl Roth, Karlsruhe, Germany) according to the manufacturers description. 50 µl of each refolded sample was used for an activity test using naringenin as substrate (3.6.3). The reactions were incubated over night and stopped by the extraction method. However, before the actual extraction 1 µl of anthracene-9-carboxylic acid (AC-9) was added as internal standard. The samples were analyzed by high-performance liquid chromatography (HPLC).

8

9 **Assessment of refolding performance**

10 The performance of each buffer on the refolding of SOMT-2 was examined by
11 comparing the SDS-PAGE results, as well as the amount of soluble protein and the
12 conversion of substrate. Main effects were analyzed qualitatively using main effects
13 plots [12].

14 **Upscaling of refolding reactions**

15 Refolding reactions were scaled up to 50 ml. Therefore 2.5 ml solubilized SOMT-2
16 (1 mg/ml) were added over 10 minutes to 50 ml of refolding buffer while stirring at
17 RT. The refolding reaction was allowed to complete over night at 4 °C.

18 **3.4.12 Enzymatic production of SAM and SAE**

19 SAM and SAE were prepared according to the method described by Dippe, et. al
20 [24].

21 Preparative reactions (20 ml) were performed in 0.1 M Tris/HCl, 20 mM MgCl₂,
22 200 mM KCl pH 8.0 and contained 7.5 mM adenosine triphosphate (ATP), 10 mM
23 D,L-methionine or D,L-ethionine, for the production of SAM or SAE respectively,
24 and 0.2 U S-adenosylmethionine synthase (SAMS) variant I317V. The reaction was
25 stopped by lowering the pH to 4 using 10 M acetic acid after 18 h of incubation
26 at 30 °C, 60 rpm. After 10 min incubation on ice the solution was centrifuged
27 (15 000 × g, 10 min) to remove insoluble matter. The supernatant was transferred to
28 a round bottom flask, frozen in liquid nitrogen and lyophilized.

1 Crude products were extracted from the pellet using 73 % ethanol and purified

using ion exchange chromatography (IEX). IEX was performed on a sulfopropyl sepharose matrix (25 ml) via isocratic elution (500 mM HCl). Before injection, the crude extract was acidified to 0.5 M HCl using concentrated hydrochloric acid. After elution, the product containing fractions were dried via lyophilization. The amount of product was determined by UV/VIS-spectroscopy at 260 nm using the published extinction coefficient of SAM ($\epsilon_0 = 15\,400\,M^{-1}\,cm^{-1}$) after resuspension in water [105].

3.5 Crystallographic Procedures

3.5.1 Crystallization of proteins

Commercially available crystallization screens were used to find initial crystallization conditions. The tested screens included kits available from Hampton Research (Aliso Viejo, USA) and Jena Bioscience (Jena, Germany). Crystallization screens were processed in 96-well micro-titer plate (MTP)s, where each well possessed 4 subwells aligned in a 2×2 matrix. The subwells were divided into 3 shallow wells for sitting drop vapour diffusion experimental setups and a fourth subwell, which was deep enough to act as buffer reservoir. This way the performance of each crystallization buffer could be assessed using three different protein solutions with varying concentrations, effectors etc. A pipetting robot (Cartesian Microsys, Zinsser-Analystik; Frankfurt, Germany) was used to mix 200 nl of each, protein and buffer solution, for a final volume of 400 nl. The crystallization preparations were incubated at 16 °C and the progress of the experiment was documented by an automated imaging-system (Desktop Minstrel UV, Rigaku Europe, Kent, UK). Furthermore, fine screens (e.g. for refinement of crystallization conditions) were set up by hand in 24-well MTPs using the hanging drop vapour diffusion method.

PFOMT

PFOMT protein was concentrated to (6 to 8) mg/ml and rebuffered to 10 mM Tris/HCl pH 7.5 using Amicon® Ultracel centrifugal concentrators (10 kDa MWCO). The concentrated protein solution was centrifuged at 14 000 × g, 4 °C for 10 min

to remove any insoluble material or aggregates. Flavonoids and phenylpropanoid substrates were added to the protein solution from 10 mM stock solution in dimethyl sulfoxide (DMSO). Crystallization screens were set up as described above. *apo*-PFOMT was crystallized using the following conditions – 2 M $(\text{NH}_4)_2\text{SO}_4$, 20 % glycerol. The protein solution contained 0.25 mM SAE, 0.25 mM MgCl_2 , 0.25 mM eriodictyol and 7.53 mg/ml (0.262 mM) PFOMT .

BWEIGEL: ist das korrekt?

8 Crystallization of proteins using NADES

NADES have the potential to be excellent solvents for hydrophobic compounds such as flavonoids or cinnamic acids [18] and in addition they are able to stabilize and activate enzymes [44].

BWEIGEL: To introduction

Four different model proteins (bovine trypsin, hen-egg white lysozyme, proteinase K and *Candida cylindrica* lipase B) were used to assess the capability of NADES for protein crystallization. PCH was tested in a full factorial grid laying out using PCH concentrations of (20, 30, 40 and 50) % combined with buffers of different pH. The buffers included 0.1 M sodium acetate pH (4.5 and 5.5), 0.1 M sodium citrate pH 6.5, 0.1 M 2-[4-(2-hydroxyethyl)piperazin-1-yl]ethanesulfonic acid (HEPES)/NaOH pH (7 and 7.5) and 0.1 M Tris/HCl pH 8.5. Thus, the full factorial design had a size of $4 \times 6 = 24$ different conditions. Protein solutions were prepared from lyophilized protein and were as follows: 90 mg/ml trypsin in 10 mg/ml benzamidine, 3 mM CaCl_2 ; 75 mg/ml lysozyme in 0.1 M sodium acetate pH 4.6; 24 mg/ml proteinase K in 25 mM Tris/HCl pH 7.5 and 6 mg/ml lipase B in water. For crystallization 2 μl enzyme solution and 1 μl reservoir buffer were mixed and set up in a hanging drop experiment on a 24-well MTP. The experiments were set up at 4 °C.

26 3.5.2 Data collection and processing

Crystallographic data were collected at the beamline of the group of Professor Stubbs (MLU, Halle, Germany). The beamline was equipped with a rotating anode X-ray source MicroMax007 (Rigaku/MSC, Tokio, Japan), which had a maximum power of 0.8 kW (40 kV, 20 mA) and supplied monochromatic Cu-K_α -radiation with

² a wavelength of 1.5418 Å. Diffraction patterns were detected with a Saturn 944+
³ detector (CCD++, Rigaku/MSC, Tokio, Japan).

⁴ Indexing and integration of the reflexes via Fourier transformation (FT) was accom-
⁵ plished using *XDS* [51, 50, 52] or *MOSFLM* [90]. *Scala* [31], which is integrated in
⁶ the Collaborative Computational Project No. 4 (CCP4)-Suite, was used for scaling
⁷ of the intensities.

⁸ 3.5.3 Structure solution

⁹ For the determination of the electron density $\rho(\mathbf{r})$, where \mathbf{r} is the positional vector,
¹⁰ from the diffraction images by FT two terms are necessary as coefficients; the
¹¹ *structure factor amplitudes*, $F_{\text{obs}}(\mathbf{h})$ and the *phase angles* or *phases*, $\alpha(\mathbf{h})$, where \mathbf{h}
¹² is the reciprocal index vector. The structure factor amplitudes can be directly
¹³ determined from the measured and corrected diffraction intensities of each spot.
¹⁴ However, the phase information is lost during the detection of the diffracted photons
¹⁵ and there is no direct way to determine the phases. This constitutes the so-called
¹⁶ *phase problem*. Thus, additional phasing experiments are necessary in order to
¹⁷ obtain the phases. A variety of phasing experiments are available, which include
¹⁸ *marker atom substructure methods*, *density modification* and *molecular replacement*
¹⁹ (*MR*) techniques [97]. Phases of the structures herein were exclusively determined
²⁰ by *MR* [94, 95].

²¹ *MR* was performed using the software *Phaser* [78, 79], which is included in the
²² CCP4-Suite [124]. A previously published PFOMT structure (PDB-code: 3C3Y [57])
²³ was used as a template during *MR* procedure for the PFOMT structure solution.

²⁴ For the *MR* of the lysozyme structure the PDB-entry 4NHI was used.

BWEIGEL: Lysozym struktur

²⁵ 3.5.4 Model building, refinement and validation

²⁶ Macromolecular model building and manipulation, as well as real space refine-
²⁷ ment and Ramachandran idealization were performed using the Crystallographic
²⁸ Object-Oriented Toolkit (*Coot*) software [29]. Structure refinement was done us-
²⁹ ing the software REFMAC5 [83, 116] as part of the CCP4-suite or the Phyton-
based Hierarchical Environment for Integrated Xtallography (PHENIX) [1]. Vali-

dation of the structures was carried out using the web service MolProbity (<http://molprobity.biochem.duke.edu/>) [16]. Structure visualization and the preparation of figures was performed using PyMOL (Schrödinger, New York, USA).

3.5.5 *In silico* substrate docking

In silico molecular docking studies were performed using the AutoDock Vina 1.1.2 or AutoDock 4.2.6 software in combination with the AutoDockTools-Suite (<http://autodock.scripps.edu/>) [45, 81, 115]. Substrates were docked into the PFOMT structure with the PDB-code 3C3Y. The grid box, which determines the search space, was manually assigned to center at 1.581, 5.196 and 25.718 (x, y, z) and had size of (22, 20 and 25) Å (x, y, z). The exhaustiveness of the global search for AutoDock Vina was set to 25, whereas the rest of the input parameters were kept at their defaults.

3.6 Analytics

3.6.1 Recording of growth curves

Starter cultures (\approx 2 ml) of the transformed *E. coli* cells were prepared in the medium to be studied, containing the appropriate antibiotics. The cultures were incubated at 37 °C, 200 rpm over night and harvested by centrifugation (5000 $\times g$, 4 °C, 5 min). The pellet was resuspended in 15 ml PBS and the suspension centrifuged (5000 $\times g$, 4 °C, 5 min). The supernatant was discarded and the washing step repeated once more. The washed pellet was resuspended in 2 ml of the medium to be studied with the appropriate antibiotics and the OD⁶⁰⁰ was measured. Three independent 50 ml cultures of the medium containing the appropriate antibiotics were inoculated such that OD⁶⁰⁰ \approx 0.05 using the washed cell suspension. The cultures were incubated at the conditions to be studied and sampled at appropriate intervals of time (\approx 1 h). One ml samples were kept on ice until all samples were acquired. 100 µl aliquots of the samples were transferred into a clear MTP and the OD⁶⁰⁰ was measured.

Green fluorescent protein (GFP) fluorescence was measured accordingly, but the

² MTP used was opaque. Excitation (λ^{ex}) and emission (λ^{em}) wavelengths were (470
³ and 510) nm respectively.

⁴ 3.6.2 *In vitro determination of glucose*

⁵ The glucose concentration in clarified, aqueous samples was determined by a mod-
⁶ ified version of the glucose assay kit procedure provided by Sigma-Aldrich [107].

⁷ Glucose oxidase (GOD) oxidizes D-glucose to gluconic acid, whereby hydrogen
⁸ peroxide is produced. The hydrogen peroxide can be detected and quantified by
⁹ horseradish peroxidase (HRP), which reduces the produced H₂O₂ and thereby oxi-
¹⁰ dizes its chromogenic substrate *o*-dianisidine via consecutive one-electron transfers.

¹¹ The oxidized diimine form of *o*-dianisidine can then be measured photospectro-
¹² metrically [17].

¹³ The methodology employs a coupled photospectrometric assay using GOD and HRP
¹⁴ with *o*-dianisidine as reporter substrate. The assay was prepared in MTP-format.

¹⁵ A reaction solution containing 12.5 U/ml GOD, 2.5 U/ml HRP and 0.125 mg/ml *o*-
¹⁶ dianisidine dihydrochloride in 50 mM sodium acetate pH 5.1 was prepared.

¹⁷ Sample solutions from culture supernatants were typically diluted in 9 volumes of
¹⁸ water. The reaction was started, by adding 50 µl reaction solution to 25 µl of sample
¹⁹ and was incubated at 37 °C and 200 rpm for 30 min in a shaking incubator. 50 µl
²⁰ 6 M sulfuric acid was added to stop the reaction and achieve maximum color devel-
²¹ opment (full oxidation of any *o*-dianisidine charge transfer complexes) (Figure 3.1).

²² The developed pink color was measured at 540 nm in a MTP-reader. A calibration
²³ curve of a standard D-glucose solutions (0 to 100 µg/ml), that was always part of
²⁴ the experiments, was used to quantify the sample measurements.

²⁵ 3.6.3 *In vitro O-methyl transferase (O-MT) assay*

²⁶ O-methyl transferase (O-MT) assays were conducted in a total volume of (50
²⁷ to 100) µl. The standard assay buffer was 100 mM Tris/HCl, 2.5 µM GSH pH 7.5.

²⁸ 1 mM MgCl₂, which was otherwise omitted, was added for reactions using cation
²⁹ dependent O-MTs (e.g. PFOMT). Reactions contained 0.5 mM alkyl donor (e.g. (S,S)-
SAM) and 0.4 mM flavonoid or cinnamic acid substrate. Enzymatic reactions were

BWEIGEL: nochmal auseinanderklamüsern wegen den konzentrationen und eingesetzten enzymmengen...

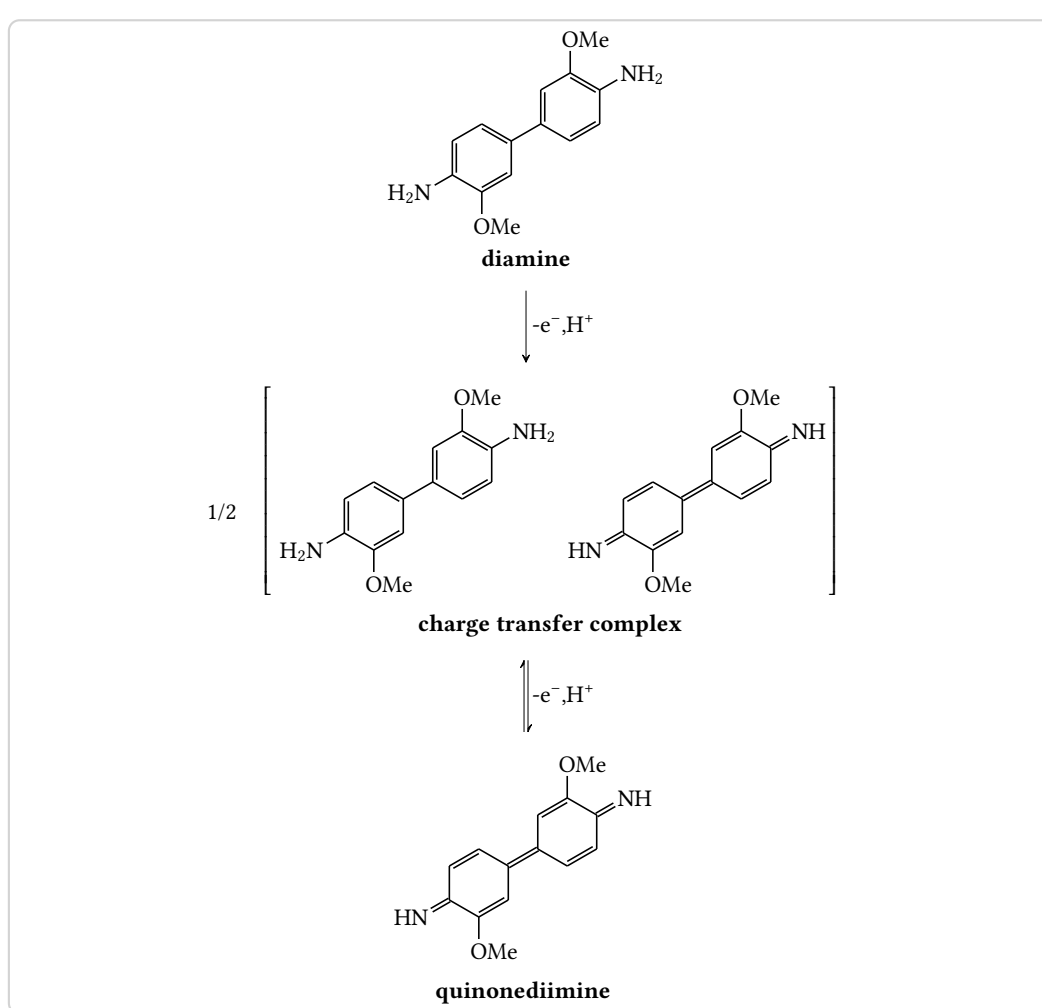


Figure 3.1: Oxidation of the reporter substrate *o*-dianisidine. Consecutive one-electron transfers lead to the fully oxidized diimine form of *o*-dianisidine. The first electron transfer is believed to produce a charge transfer complex intermediate. [49, 17]

² started by addition of enzyme (usually 0.2 mg/ml) and incubated at 30 °C.
³ Reactions were stopped by addition of 500 µl ethyl acetate containing 2 % formic acid
⁴ and vortexed for 15 s to extract the hydrophobic phenylpropanoids and flavonoids.
⁵ After centrifugation (10 000 × g, 4 °C, 10 min) the organic phase was transferred
⁶ into a new tube. The reaction was extraced once more with 500 µl ethyl acetate,
⁷ 0.2 % formic acid and the pooled organic phases were evaporated using a vacuum
⁸ concentrator (Concentrator 5301; eppendorf, Hamburg, Germany). The residue was
⁹ dissolved in methanol and centrifuged at 10 000 × g for 10 min to remove unsoluble
¹⁰ matter. The supernatant was transferred into a HPLC vial and analyzed by HPLC
¹¹ (3.6.8).
¹² When detection of hydrophobic (e.g. flavonoids) and hydrophilic compounds (e.g.
¹³ SAM, SAH) was performed simultaneously reactions were stopped by addition of
¹⁴ 0.3 volumes 10 % (w/v) TCA in 50 % acetonitrile. The mixture was vortexed for
¹⁵ complete mixing and incubated on ice for at least 30 min. After centrifugation
¹⁶ (10 000 × g, 4 °C, 10 min) the supernatant was transferred into HPLC-sample vials
¹⁷ and analyzed (see 3.6.8).

¹⁸ Measurement of activity/pH profiles

¹⁹ Assays to measure activity over larger pH ranges were set up in 50 mM L-malic
²⁰ acid/MES/Tris (MMT)- (pH 4 to 9) or succinate/sodium phosphate/glycine (SSG)-
²¹ buffer (pH 4 to 10) to keep the concentrations of buffer salts constant for each pH
²² [84].

²³ The protein of interest was first extensively dialyzed against the reaction buffer
²⁴ (e.g. MMT, SSG) at pH 7 with added EDTA (5 mM) and then against the same
²⁵ buffer without EDTA. Standard reaction conditions were 50 mM buffer, 0.4 mM
²⁶ alkyl acceptor (e.g. caffeic acid), 0.5 mM SAM, 2.5 µM GSH and 0.2 mg/ml enyzme.
²⁷ MgCl₂ was either omitted or added at 10 mM to assess influences of divalent cations.
¹ Assays were stopped as described in 3.6.3 and analyzed accordingly.

3.6.4 Photospectrometric assay for the methylation of catecholic moieties

Catecholic moieties can form stable complexes in the presence of heavy metals such as copper or iron [103, 80]. Hence, caffeic acid can complex ferric (Fe^{3+}) ions and form a colored complex with $\lambda_{\text{max}} = 595 \text{ nm}$ [23]. Since the complex formation is specific for caffeic acid and methylated derivatives (i.e. ferulic and iso-ferulic acid) cannot complex Fe^{3+} , this can be used as a measure for methylation reactions. O -MT assays were prepared as before (3.6.3). However, the reactions were stopped by addition of 0.1 volumes 1 M Tris/HCl pH 8, immediately followed by 0.5 volumes catechol reagent (2 mM FeCl_3 in 10 mM HCl). The complex formation reaction was allowed to equilibrate for 5 min at RT and the absorbance at 595 nm was measured.

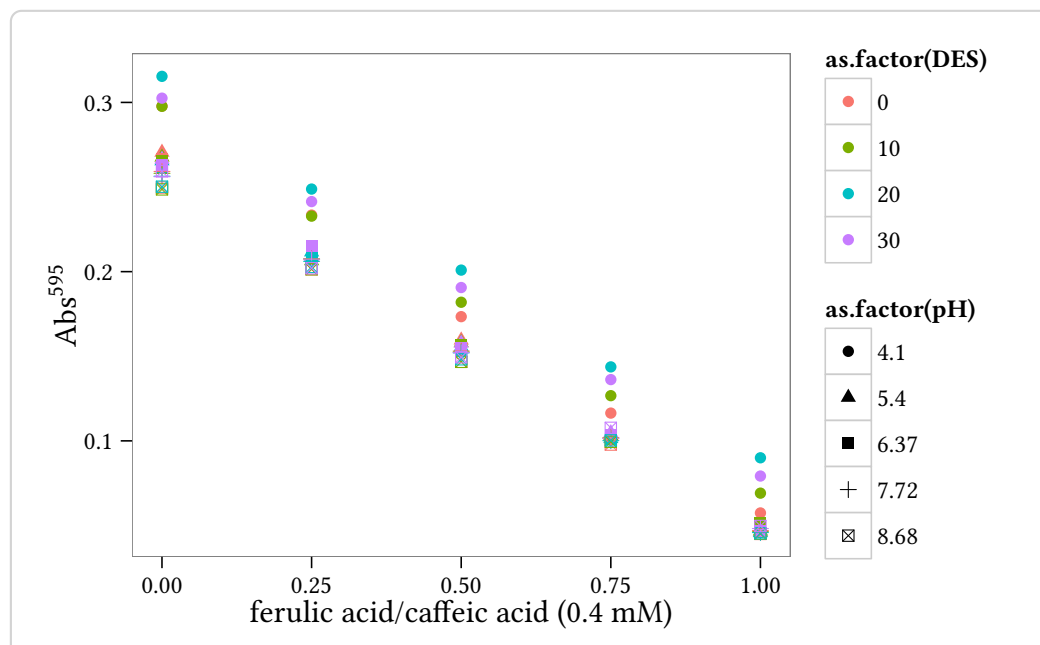


Figure 3.2: Calibration curves of different relative compositions of ferulic acid to caffeic acid, that were taken as described in 3.6.4. The total concentration was always 0.4 mM. At lower pH values around 4, the method seems to overestimate the concentration of caffeic acid. However, the slope of the curves stays the same.

3.6.5 Concentration of SOMT-2 using hydrophobic interaction chromatography (HIC)

After refolding using rapid dilution protein samples are very dilute and a concentration step is required. Refolded SOMT-2 was concentrated directly from the refolding buffer using hydrophobic interaction chromatography (HIC).

The ammonium sulfate concentration of the protein sample was brought to 1 M using a 2 M $(\text{NH}_4)_2\text{SO}_4$ solution and the pH was adjusted to 7 using 5 M NaOH. The sample was centrifuged ($20\,000 \times g$, 4°C , 30 min) to remove insoluble material and the clarified supernatant was applied to a 1 ml HiTrap Phenyl FF (Low Sub) (GE Healthcare, Freiburg, Germany), which had been equilibrated with high salt buffer (1 M $(\text{NH}_4)_2\text{SO}_4$, 50 mM HEPES pH 7). The target protein was eluted using a stepwise gradient ((1, 0.8, 0.6, 0.4, 0.2 and 0) M $(\text{NH}_4)_2\text{SO}_4$, 50 mM HEPES pH 7; 5 CV each) to remove the ammonium sulfate. The column was washed using 20 % ethanol. Before SDS-PAGE analysis the eluted high salt fractions were desalted using TCA precipitation (3.4.4).

3.6.6 Analytical gel filtration

Analytical gel filtration was done using a Superdex 200 10/300 GL column (GE Healthcare, Freiburg, Germany) in combination with a FPLC system according to the manufacturers instructions. The column was equilibrated using an appropriate buffer (e.g. 0.1 M Tris/HCl pH 7.5) and 100 μl of sufficiently concentrated ($\geq 1 \text{ mg/ml}$) protein sample were injected. The Gel Filtration Standard by Bio-Rad (München, Germany) was run separately to assess the size of the proteins in the analyzed sample.

3.6.7 Binding experiments using Isothermal Titration Calorimetry (ITC)

ITC can be used to directly characterize the thermodynamics of an observed process, be this a binding interaction or an enzymatic reaction [32].

ITC measurements to describe the interaction between PFOMT and its substrates/-

effector where performed using a MicroCal iTC200 device (Malvern, Worcestershire, UK). PFOMT protein was extensively dialyzed against 50 mM MMT-buffer pH 7 prior to ITC experiments. The solution was subsequently centrifuged ($14\,000 \times g$, 4 °C, 10 min), to remove insoluble matter and aggregates. The dialysate was stored at 4 °C and used to prepare substrate and effector solutions. Generally 50 µM protein was provided in the ITC cell and the effectors/substrates to be titrated were loaded into the syringe. The substance concentration in the syringe was ten times higher than the protein solution. Experiments were carried out at 20 °C unless otherwise stated. The stirring speed was set to 500 rpm. The injection volume was set to (2 to 4) µl, amounting to a total of 10 to 19 injections.

3.6.8 High-performance liquid chromatography (HPLC) analytics

Due to their aromaticity, methanolic extracts of flavonoids exhibit two major absorption peaks in the UV/VIS region of the light spectrum in the range of (240 to 400) nm [72]. However, even the more simple phenyl propanoids (e.g. cinnamic acids) show absorption of light in the UV/VIS-region.

Methanolic extracts of flavonoids and phenyl propanoids were analyzed by HPLC using a photo diode array (PDA)-detector, which was set to record in the range of (200 to 400) nm. HPLC runs were performed on a reverse-phase C-18 end-capped column (YMC-Pack ODS-A; YMC Europe, Dinslaken, Germany) with a pore size of 120 Å. The mobile phase was aqueous acetonitrile supplemented with 0.2 % formic acid. The flow was kept constant at 0.8 ml/min. 10 µl O-MT enzyme assay extract (3.6.3) were injected and analyzed using an acetonitrile gradient starting with 5 % acetonitrile (4 min). The acetonitrile content was increased to 100 % in 21 min and was kept at 100 % for 5 min. Peaks were integrated from the 280 nm trace using the software provided by the manufacturer of the device.

3.6.9 liquid chromatography coupled mass-spectrometry (LC/MS) measurements

4 Evaluation of PFOMT towards the acceptance of long-chain SAM analogues

4.1 Introduction

⁶ Small changes to molecules can have profound influences on their chemical, physicochemical and biological properties. Butyric acid esters differing only by a few methylene groups already exhibit quite divergent smells. However, not only the macroscopically qualitative properties can differ. The quantifiable psychotomimetic effect of methylated and ethylated lysergic acid amids differ by at least an order of magnitude [106, 42]. There are many more of these so-called structure activity relationships (SARs) and quantitative structure activity relationships (QSARs) studies on any number of compounds and situations [100, 4, 75].

¹⁴ Methylation reactions are one of the key tailoring steps during natural product biosynthesis and can in consequence greatly affect a molecule's bio- and physicochemical behaviour [111, 62]. However, between the highly complex core structures of natural products, which are produced by a plethora of enzymes (e.g. poly ketide synthases (PKSs), non-ribosomal peptide synthases (NRPSs), terpene cyclases), and the rather simple alkyl-modification introduced by methylation nature is missing some medium-sized modification options, that proceed as elegantly as the methylation by MTs. Thus, natural products containing longer chain alkyl modifications

Chapter 4. Evaluation of PFOMT towards the acceptance of long-chain SAM analogues

4.1. Introduction

like ethyl or propyl moieties on O, N or S-centers have rarely, if ever been observed.¹

It has recently been shown however, that a wide array of SAM analogues are used as co-substrates by a variety of MTs [111]. The majority of the work so far has been done on P-MTs and DNA MTs (Figure 4.1), since epi-genetics and finding regions of gene-reulation is of great interest. There have been a great many of SAM analogues synthesized, both chemically and with the help of enzymes [19, 108].

8

However, the first description of novel synthetic SAM analogues with extended carbon chains, including SAE, allyl and propargyl derivatives, that were also shown to be useful in modifying DNA via the action of several DNA MTs was provided by Dalhoff, *et al.* [19, 20]. It was also noted, that allyl transalkylation reactions proceeded much faster than ethyl- or propyl transfers possibly due to conjugative stabilization of the transition state [19]. A whole variety of allyl derivatives was examined by different researchers and site-specific introductions of allyl, pent-2-en-4-ynyl and even 4-propargyloxy-but-2-enyl moieties into proteins (i.e. histones) was demonstrated using P-MTs [121, 89]. However, the larger substrate analogues were not necessarily accommodated by the native P-MTs making engineering efforts for the accommodation of larger substrates inevitable [121]. The specific introduction of alkine functionalized groups made it then possible to use click chemistry for further functionalization and/or detection of the labelled proteins, DNA or RNA and has been studied extensively (Figure 4.2) [121, 89, 82, 123, 101].

In 2012 Bothwell and Luo even described the exchange of the sulfonium with a selenonium center, which afforded SeAM analogues that have since then been described as substrates for several P-MTs [11, 10]. SeAM analogues have the advantage of being more resistant to chemical decomposition than their sulfur counterparts, but also show enhanced transmethylation reactivity [10].

There have also been some reports on the use of SAM analogues by small molecule MTs. In 2009 Stecher *et al.* reported the use of the C-methyl transferases (C-MTs) NovO and CouO along with synthetic SAM analogues to accomplish biocatalytic

¹Reaxys searches for natural product isolates with a molecular mass between (150 and 1500) containing the substructures methyl, ethyl or propyl connected to a heteroatom return 66759, 2797 and 52 results respectively. However, it stands to note that 70 % of the propyl results were either esters or otherwise activated moieties. [28]

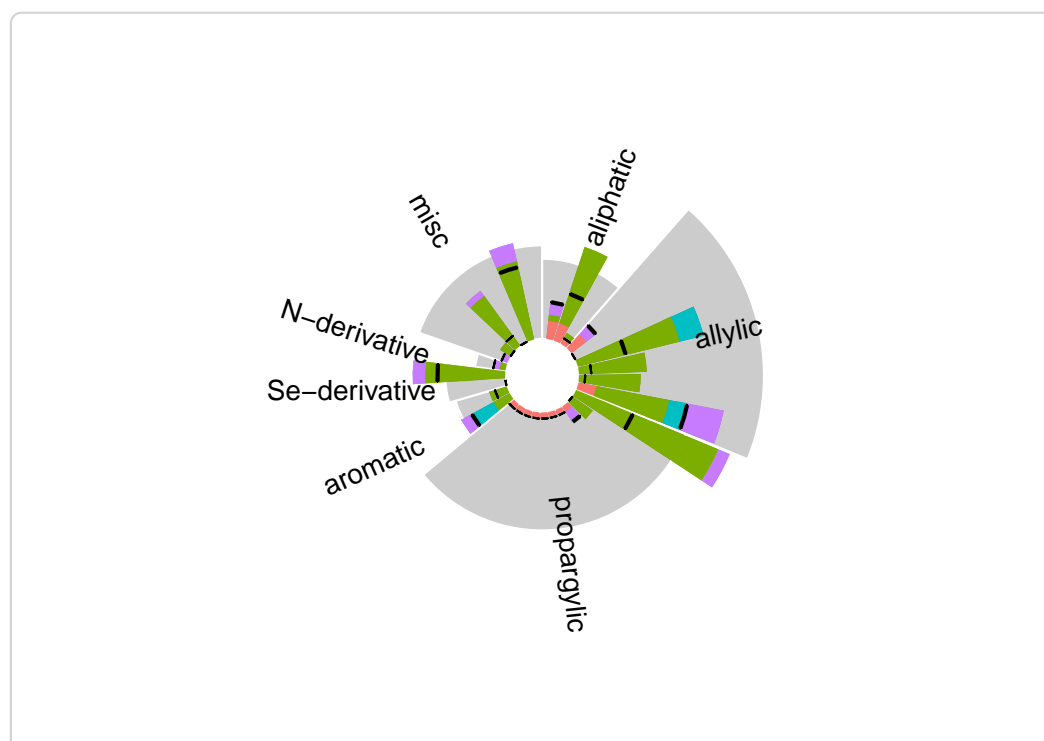


Figure 4.1: Graphical representation of the work that has been done on MTs in combination with SAM analogues. The grey areas represent individual groups of SAM analogues (aliphatic, allylic, propargylic, aromatic, SeAM analogues, nitrogen analogues and miscellaneous others). The height of the grey areas represents the number of times a member of the corresponding group has been described as tested in the MT literature. The height of the colored bars represents the times that individual substrate has been tested. The colors represent the different types of MT (red – DNA MT, green – P-MT, lilac – small molecule MT, blue – rna MT). The black dash across the bar shows the number of times this substrate was actually converted by either enzyme.

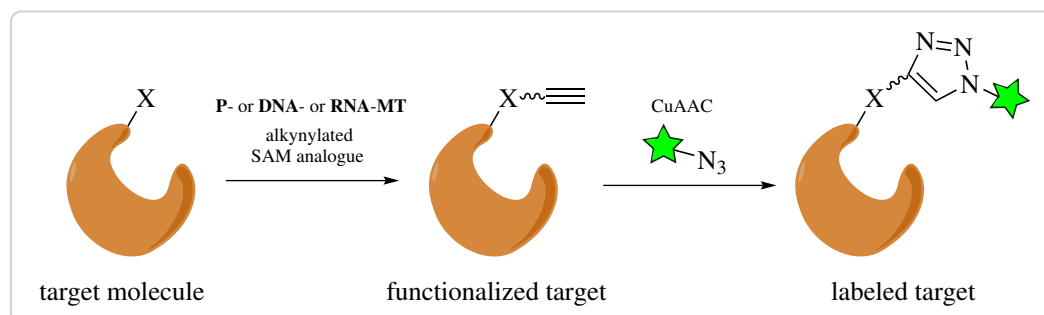


Figure 4.2.: Labelling of macromolecules by using a combination of novel alkyne-derivatized SAM analogues and Cu^I -catalyzed azide-alkyne 1,3-dipolar cycloaddition (CuAAC). Depending on the type of label used, it can be employed for detection (e.g. through fluorophores, coupled assays) or affinity purification (e.g. biotin). This technique is also feasible for use in activity based protein profiling (ABPP) approaches.

² Friedel-Crafts alkylations of some aminocoumarine antibiotics [109]. Lee *et al.* were
³ the first ones to describe the transfer of a keto-group from an SAM derivative
⁴ by means of the small molecule MTs catechol *O*-methyl transferase (EC 2.1.1.6)
⁵ and thiopurine *S*-methyl transferase (EC 2.1.1.67) [61]. Furthermore there was
⁶ work done on the *O*-MTs RebM and RapM, which modify the antitumor active
⁷ natural products rebeccamycin and rapamycin respectively, that shows the general
⁸ feasibility of using SAM analogues in combination with MTs to modify small
⁹ molecules [60, 108, 127]. In all of these reports the specificity of the group transfer
¹⁰ is retained despite the fact that SAM analogues are employed as substrates.

¹¹ There is of yet no bioactivity data reported that shows the biological activity of the
¹² newly produced compounds.

¹³ PFOMT is highly promiscuous towards its flavonoid substrate [57, 46]. However,
¹⁴ the promiscuity towards different SAM analogues has not yet been described.
¹⁵ Combination of both, substrate and co-substrate promiscuity in the small molecule
¹⁶ MT PFOMT could provide a powerful tool towards the biosynthetic production
¹⁷ of novel small molecules with potentially new and promising biological activities.
¹⁸ Functionalization/Detection of substrates could furthermore provide a means of
¹⁹ finding new compounds/substrates in complex (e.g. biological) samples analogous
²⁰ to activity based protein profiling (ABPP) approaches. It was thus of interest,
¹ whether or not PFOMT would accept SAM analogues as alkyl donors. The already

extensively studied PFOMT was the prime candidate, since the preparation and crystallizability were established and lots of substrates had already been described [117, 46, 57, 13].

4.2 In silico docking studies using computational tools

Prior to any experimental techniques different known and potential substrates were docked to PFOMT using molecular modelling.

BWEIGEL: entweder noch machen oder raus damit

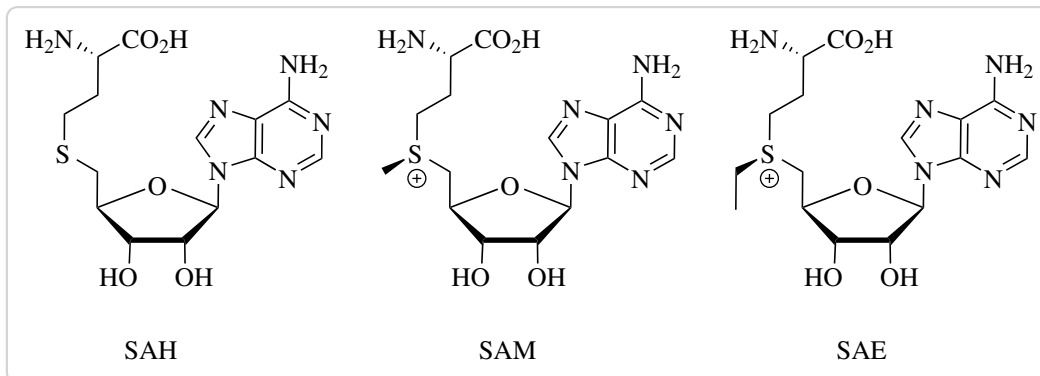


Figure 4.3.: The binding of different SAM analogues was measured via ITC, but also calculated using molecular modelling techniques.

4.3 Substrate binding studies using ITC

The binding of different substrates by PFOMT was examined by ITC. SAH, SAM and SAE were selected to study the influence of the alkyl chain length on binding. Furthermore the binding of the substrate caffeic acid and the influence of Mg²⁺ addition on substrate binding was investigated.

The K_D values of SAH, SAM and SAE were all in the low micromolar range, around 2 μM. However, the binding enthalpy clearly decreased with the length of the aliphatic chain connected to the sulfur atom (Figure 4.4a). The binding of

² SAH, gave off more heat than the binding of SAM, which in turn gave off more
³ heat than the binding of SAE. Thus, the entropic influence must get larger with
⁴ increasing chain length in order for (4.1) and (4.2) to still hold true. Indeed, the
⁵ value for ΔS was negative for binding of SAH and got positive for the binding of
⁶ SAM and SAE (Table ??). This relationship between the change of entropy and
⁷ the change of enthalpy has been found for many biological systems and is also
⁸ called enthalpy-entropy compensation (EEC) [104, 38, 26]. The stoichiometry
⁹ for the binding process is given by the parameter N (Table ??). For all the ligands
¹⁰ SAH, SAM and SAE this value was found to be about 0.5, which corresponds to
¹¹ one bound molecule ligand per dimer of PFOMT.

¹² Upon titration of caffeic acid to PFOMT small amounts of heat were given off
¹³ by the system (Figure 4.4c). When the enzyme was incubated with SAH prior to
¹⁴ addition of caffeic acid this heat increased slightly. The slope of the ITC profile
¹⁵ also got steeper. However, the data obtained could not be fitted to afford a sensible
¹⁶ solution. When caffeic acid and Mg^{2+} were incubated with PFOMT prior to addition
¹⁷ of SAH, the process of heat production as observed by ITC also had a steeper slope.
¹⁸ Nonetheless, the thermodynamic parameters did not differ significantly. On its
¹⁹ own Mg^{2+} , in the form of an $MgCl_2$ solution, titrated to the enzyme solution did
¹ not cause signals during the ITC experiments.

$$\Delta G = \Delta H - T\Delta S \quad (4.1)$$

$$\Delta G = \Delta G^0 - RT \ln K \quad (4.2)$$

Table 4.1: Results of fitting a simple one-site binding model to the data obtained from ITC experiments.

	K_D [μM]	ΔH [cal mol $^{-1}$]	ΔS [cal mol $^{-1}$ K $^{-1}$]	N
SAH	2.06 ± 4.27	$-10\,380 \pm 1025$	-9.41	0.505 ± 0.038
SAM	1.08 ± 3.50	-4606 ± 242	11.6	0.492 ± 0.018
SAE	2.22 ± 3.79	-1338 ± 190	21.3	0.513 ± 0.050

Chapter 4. Evaluation of PFOMT towards the acceptance of long-chain SAM analogues

4.3. Substrate binding studies using ITC

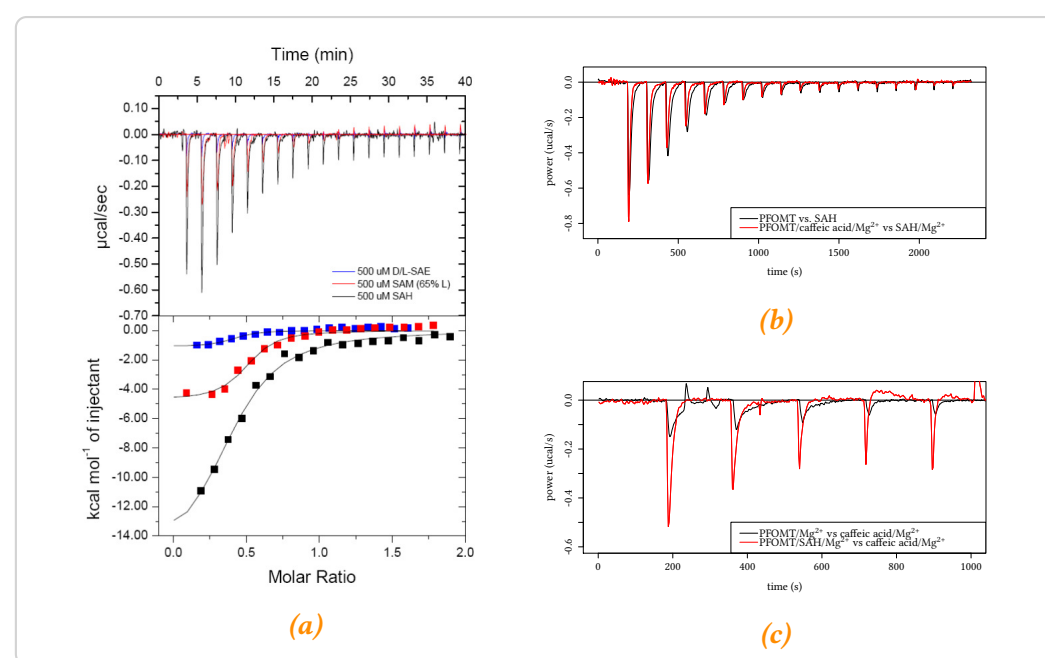


Figure 4.4.: Exemplary ITC measurements. **a** – Binding of SAH, SAM and SAE to PFOMT. **b** – SAH is injected into a PFOMT solution, with (red) or without (black) addition of Mg^{2+} and caffeic acid. When Mg^{2+} and caffeic acid were already present, the binding process seems to happen quicker, but is less enthalpic. **c** – Upon addition of caffeic acid to the protein heat is produced, however no sensible binding curve could be obtained.

4.4 Study of variants for long-chain alkylations

³ The work described in this section was done in cooperation with Dr. Martin Dippe.

⁴ Dr. Dippe did most of the work on the PFOMT variants described herein.

⁵

⁶ Since the ability to bind the elongated analogue SAE was present in wildtype
⁷ PFOMT, the activity of the PFOMT protein was tested. Activity tests were performed
⁸ with caffeic acid as substrate under standard reaction conditions. The wildtype
⁹ of PFOMT was able to use SAE as a co-substrate for the ethylation of caffeic acid,
¹⁰ albeit the amount of detected product was very minute. The site of ethylation
¹¹ was determined by liquid chromatography coupled mass-spectrometry (LC/MS)
¹² measurements. It was found that ethylation occurs on the catecholic group, however
¹³ it could not be determined whether at the 3- or 4-position. Nonetheless it is highly
¹⁴ likely that ethylation occurs at the same position as methylation and thus the
¹⁵ product was annotated as 3-ethoxy-4-hydroxy cinnamic acid.

¹⁶ Enzyme variants were prepared to further test the ethylation reactivity of PFOMT,
¹⁷ since a number of groups were able to accomplish transalkylation with larger
¹⁸ substrates by expanding the available space in the active site [121]. Residues that
¹⁹ were exchanged were selected based upon their position in the active site and in
²⁰ relation to the substrate(s) (Figure 4.5). Fortunately a crystal structure of PFOMT
²¹ was available to help with the selection.

²² Over 20 enzyme variants were prepared to assess, whether PFOMT ethylation
²³ activity would improve over the wildtype. Be that as is may, an improved ethylation
²⁴ activity was not observed. Some of the new variants however displayed an increased
²⁵ methylation activity with the substrates caffeic acid and SAM. The methylation
²⁶ activity of some of the variants increased by over 4-fold. Interestingly most amino
²⁷ acid substitutions proved as beneficial, rather than detrimental.

²⁸ Methylation activity benifited greatly from the replacement of bulky hydrophobic
²⁹ residues by smaller and/or charged residues in the vicinity of the acceptor substrates
³⁰ (Tyr51, Trp184 and Phe198). However, this was not a general trend since the
³¹ substitutions N202W and Y51W also improved methylation activity. Looking more
³² closely at residue Tyr51, the activity enhancing effect was greatest, when the

BWEIGEL: literaturvergleich der umsäzte?

BWEIGEL: LCMS messungen?

BWEIGEL: Genauer zu den Resten...

BWEIGEL: grafik?

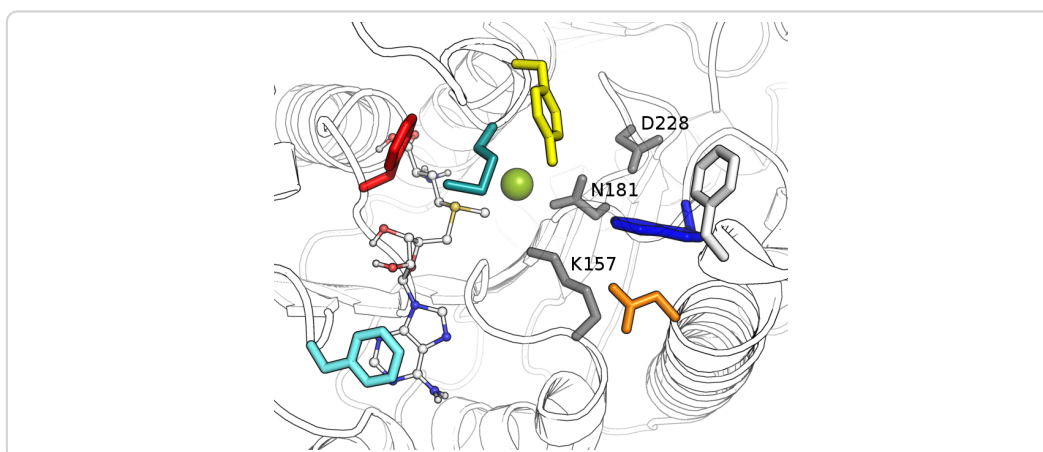


Figure 4.5.: The active site of PFOMT. The outline of the protein backbone is displayed, with active site residues portrayed as colored sticks (cyan – F103, red – F80, turquoise – M52, yellow – Y51, white – F198, blue – W184, orange – N202, grey – as labelled). The co-substrate SAM (ball-and-stick model) was docked into the structure.

tyrosine was substituted by the basic amino acids lysine or arginine. In addition to an enhanced activity the selectivity for the hydroxyl position to be methylated was also altered in these variants. This was not apparent, when caffeic acid was used as a substrate. However when a flavonoid, especially eriodictyol, was used not only the 3' hydroxyl, but to some extent the 4' hydroxyl was methylated. This effect was improved in some double variants, where also position 202 was altered. For example the variant Y51R N202W almost exclusively methylated flavonoid substrates at the 4' position . A detailed discussion of the results was published in a peer reviewed journal.

BWEIGEL: grafik? & paper

4.5 Crystallization of PFOMT

The binding of the non-natural substrate SAE to PFOMT could be shown. However, a transethylation reactivity was not observed. The question was to the chemical reasons behind these observations. Previous work on the crystal structure of PFOMT had been done, but only SAH could be co-crystallized [57]. But since the crystallizability of PFOMT had already been shown, this method was chosen to answer the aforementioned question.

At first the already crystallization procedures were evaluated to start with [57].
Albeit, reproduction of the results could not be accomplished and new crystallization conditions had to be found. This was done using commercially crystallization screening kits and a semi-automated pipetting robot along with an automated imaging system for the observation of the crystallization plates.

Each buffer solution was screened in combination with three different protein solutions (*A* – 0.25 mM SAH, 0.25 mM MgCl₂, 0.25 mM ferulic acid, 0.262 mM PFOMT; *B* – 0.25 mM SAE, 0.25 mM MgCl₂, 0.25 mM eriodictyol, 0.262 mM PFOMT and *C* – 0.25 mM SAH, 0.25 mM MgCl₂, 0.25 mM ferulic acid, 0.219 mM PFOMT Y51R N202W) to obtain protein crystals co-crystallized with the substrates.

During the preparation of the protein solutions it was noted, that upon addition of the flavonoids or phenyl propanoids from DMSO stocks these tended to precipitate. The techniques meant to circumvent this problem are discussed in chapter 7. Crystals began to appear in various wells after a few days and were observed for each tested protein solution at least once. The crystal shape varied from very smooth and almost cubic (high ammonium sulfate) over spherulites and intergrown crystals (CaCl₂, PEG-4000) to brittle and ragged needles (LiCl, PEG-6000) (Figure 4.6).

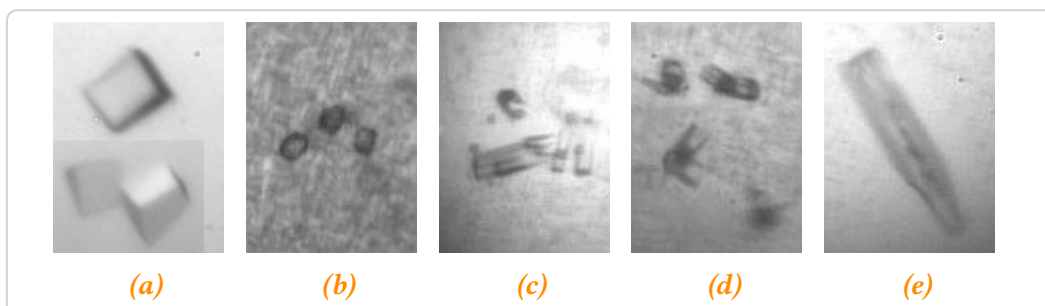


Figure 4.6.: Some crystal and pseudo-crystal shapes that were observed during the crystallization screen. *a* – high (NH₄)₂SO₄, *b-c* – CaCl₂, PEG-4000, *e* – LiCl, PEG-6000

Crystals that were large enough ($\geq 50 \mu\text{m}$), where screened for diffraction right away. A rough estimate of the resolution, cell parameters and the space group was acquired, if the diffraction images could be indexed. The screened crystals all had similar cell parameters and belonged to the same space group, *P*2₁2₁2₁. However, the unit cell of crystals that grew out of high ammonium sulfate concentrations ($\geq 1.8 \text{ M}$)

BWEIGEL: wie groß?

² was approximately four times as large as that of the published structure 3C3Y and
³ crystals that developed under different crystallization conditions. Several datasets
⁴ were collected of crystals from high $(\text{NH}_4)_2\text{SO}_4$, since these possessed different
⁵ cell parameters than the previously reported structure and therefore seemed to be
⁶ promising candidates for bound substrates.

⁷ The crystal structure of *apo*-PFOMT

⁸ Most of the collected datasets were partly solved. As it turned out however the
⁹ substrates were not co-crystallized. Rather, the *apo*-form of PFOMT had been
¹⁰ crystallized. Thus, one dataset was solved to completion to obtain a novel PFOMT
¹¹ structure with no substrate bound and a resolution of 1.95 Å (??). The assymetric
¹² unit of *apo*-PFOMT contained two homodimers (4 monomers) (Figure 4.7a), rather
¹³ than just one homodimer (3C3Y). The active site of each monomer was found to be
¹⁴ empty except for a sole sulfate ion, which was positioned where the amino- and
¹⁵ carboxylate groups of the SAH reside in the 3C3Y structure (Figure 4.7b). Shifts in
¹⁶ the structure of some loops were observed and contrary to the previously published
¹⁷ structure the entire N-terminus was resolved up to the His-tag.

¹⁸ The resolved N-terminus contained another N-terminal α -helix, which was
¹⁹ positioned in a cleft on the surface, where substrates may be bound [57]. This
²⁰ interaction extends up to the His-tag. Considerable movement was observed in
²¹ different parts of the protein, when no substrate was bound, some of which can be
²² attributed to SAM and metal ion binding residues (Figure 4.8 and Figure A.1) as is
²³ obvious for the loop region between β -sheet 1 and α -helix 4. Nonetheless, most of
²⁴ the movement seemed to be restricted to areas, which are not directly involved in
²⁵ the binding of either SAM or metal ions. However, all of the regions that moved
²⁶ are located at or near the active site.

²⁷ 4.6 Conclusion/Discussion

²⁸ Whereas the binding of SAH was solely dependent on the large negative enthalpy,
²⁹ the binding of SAE was almost entirely driven by entropy, since ΔH was close to
¹ 0 (??). Entropy gain can be a major driving force for ligand-protein interactions

BWEIGEL: mehr auf die aktuelle literatur eingehen...auch wenn sie sich i grenzen hält...

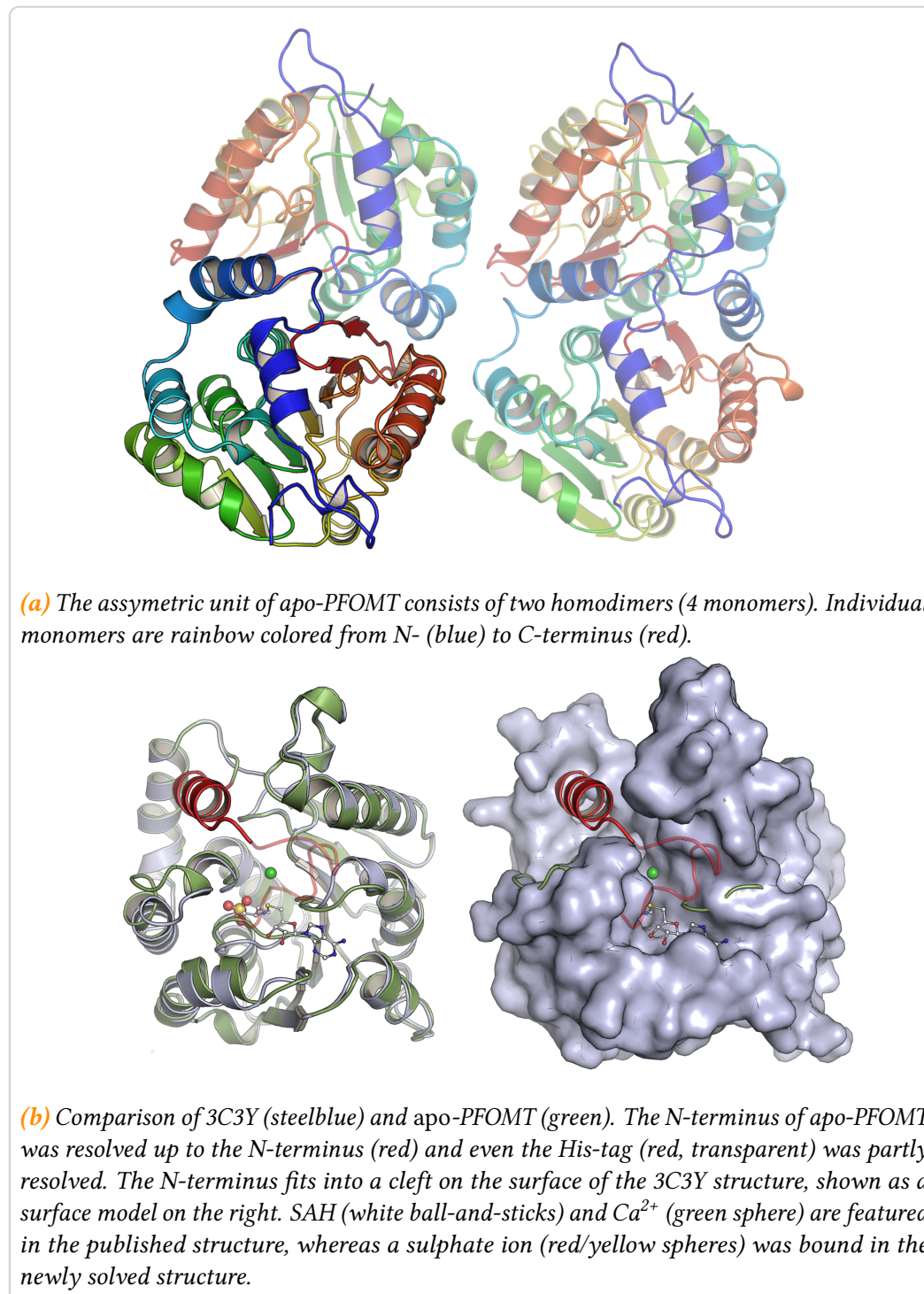


Figure 4.7: An overview of the features in the apo-PFOMT structure.

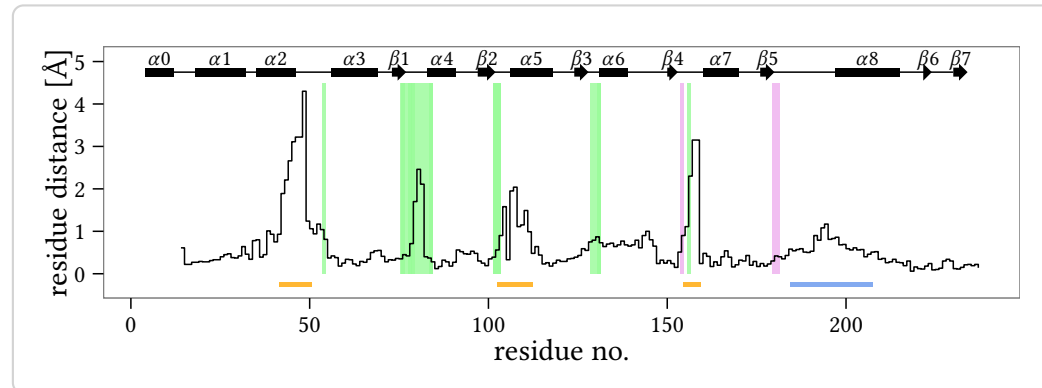


Figure 4.8: Positional differences between the individual residues of the solved apo-PFOMT and the structure with bound SAH (pdb: 3C3Y). The diffraction precision indicator [21] (DPI) of the structures was (0.137 and 0.064) Å respectively. The overall rmsd amounted to 0.9034 Å. The secondary structure of apo-PFOMT is displayed at the top. Helices are displayed as rectangles and sheets are shown as arrows. Graphical background annotations are used to display the binding sites of SAH (green) and the metal ion (plum). The orange bars indicate regions, where much movement seems to happen upon binding or release of the co-substrate. The blue bar shows the region that was annotated as "insertion loop" in previous studies [57].

and in some cases ligand binding can be entirely attributed this gain in entropy [64]. Displacement of protein-bound water molecules contributes strongly to the entropic gain. There were some waters present in the active site of PFOMT in the crystal structure developed herein. However, no metal ion was present in the active site in the *apo*-PFOMT structure. Furthermore Mg²⁺ titration via ITC did not afford significant signals, suggesting the notion, that the metal is only bound along with the co-substrate (Figure 4.9). It has been suggested, that the entropy cost to transfer one water molecule from bulk to the protein-bound state can be up to 7 cal mol⁻¹ K⁻¹ [25]. The replacement of ordered waters from the active site or from a hydrated metal ion by a growing aliphatic chain could therefore explain the gain in entropy, and SAH is positioned in a way to warrant exactly that (Figure 4.9). Also, the hydrogen and metal complexing bonds consequently lost could explain the less negative enthalpy. However, this is purely hypothetical since more evident data is missing. Additional insight might be gained by expanding the ITC experiments to even longer SAM analogues. The limited space in the active site, which forces

BWEIGEL: im buch nochmal bei comt nachlesen

Chapter 4. Evaluation of PFOMT towards the acceptance of long-chain SAM analogues

4.6. Conclusion/Discussion

the growing side chain to expel water might also be the reason for the inactivity of PFOMT towards SAE. If the metal ion is blocked from complexing moieties, activation of the substrate hydroxyl would be hindered.

Comparison of the novel *apo*-PFOMT and the published structure suggests a lot of movement along multiple parts of the backbone all proximal to the active site pocket, upon ligand binding (Figure 4.8). The N-terminus of PFOMT seems to act as a lid, which is closed in the *apo*-form, but highly flexible and therefore unresolved in the ligand bound form. Furthermore, the native enzyme has been shown to be truncated, starting only at residue 12 and being less catalytically efficient than the full length protein [117, 57]. The work presented here consequently supports the notion that the N-terminus plays an important role on the regulation of the enzymatic activity.

The laid out findings provide novel hints for regions in the PFOMT structure that can be studied using site-directed mutagenesis approaches in order to work towards a variant that can in fact employ SAE for transalkylation reactions. Furthermore variation of these regions might provide enzymes with altered substrate specificities which are of high interest.

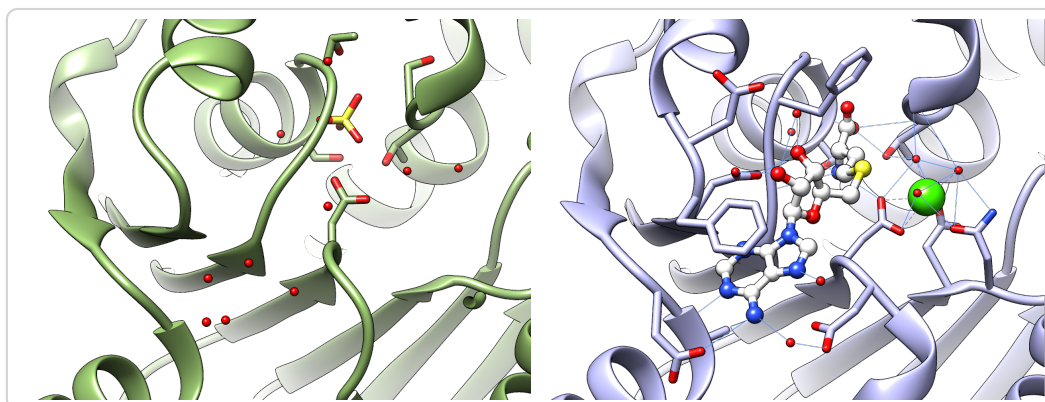


Figure 4.9: Comparison of the active sites of the apo-structure (left, green) and the ligand-bound structure (right, steelblue). Waters are represented as small red spheres, calcium as a green sphere (complexing bonds are dashed) and SAH is displayed as a white ball-and-stick model. A possible hydrogen bond network (blue lines) for the ligand-bound state is displayed.

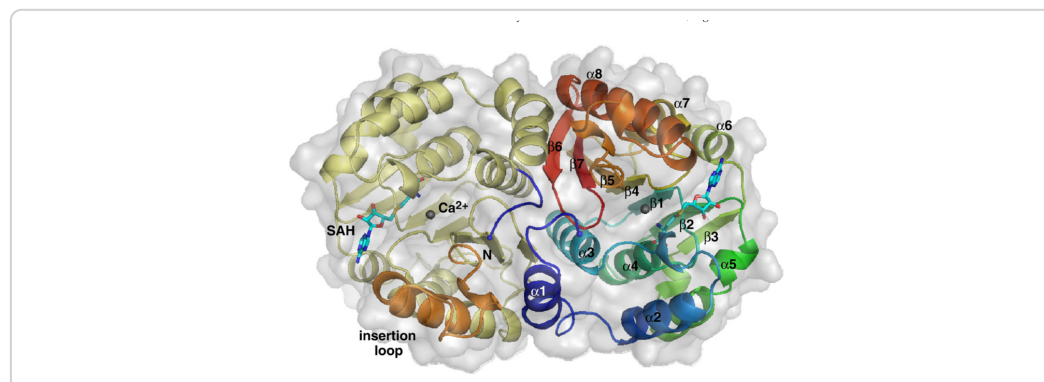


Figure 4.10: from: Kopycki, J. G., Rauh, D., Chumanovich, A. a., Neumann, P., Vogt, T., & Stubbs, M. T. (2008). Biochemical and Structural Analysis of Substrate Promiscuity in Plant Mg²⁺-Dependent O-Methyltransferases. *Journal of Molecular Biology*, 378(1), 154–164.
<http://doi.org/10.1016/j.jmb.2008.02.019>

² 5 Enzymatic methylation of Non-catechols

⁴ 5.1 Introduction

⁵ Non-catechols in nature (biosynthesis, mode of action?), chemical methylation???

⁶ 5.2 SOMT-2

⁷ 5.2.1 In vivo methylation studies using *N. benthamiana*

⁸ 5.2.2 In vivo studies in *E. coli*

⁹ 5.2.3 In vitro studies using recombinantly produced SOMT-2

¹⁰ 5.3 PFOMT

¹¹ 5.3.1 Acidity and Nucleophilicity of phenolic hydroxyl-groups

¹² 5.3.2 pH-Profiles of PFOMT-catalysis

¹³ 5.3.3 Influence of Mg²⁺ on PFOMT activity

¹⁴ 5.4 Consensus or Bioinformatic points-of-view ¹⁵ (COMT)???

5.5 Conclusion/Discussion

² **6 Development of an whole cell
methyl transferase screening sys-
tem**

⁵ **6.1 Introduction**

⁶ **6.2 Theoretical considerations / design of system**

⁷ **6.3 Detectability of *S*-adenosyl-L-homocysteine
(SAH)**

⁸ SAM

¹⁰ **6.4 Usage of the *lsr*-promoter for true autoinduc-
tion**

¹¹ **6.5 Conclusion/Discussion**

7 DES in protein crystallography

7.1 Introduction

7.2 Solubility enhancement of hydrophobic substances by addition of DES

7.3 Enzymatic *O*-methylation in DES

7.4 DES as precipitants in protein crystallization

7.5 Conclusion/Discussion

8 Acknowledgements

³ Quisque ullamcorper placerat ipsum. Cras nibh. Morbi vel justo vitae lacus tincidunt
⁴ ultrices. Lorem ipsum dolor sit amet, consectetur adipiscing elit. In hac habitasse
⁵ platea dictumst. Integer tempus convallis augue. Etiam facilisis. Nunc elementum
⁶ fermentum wisi. Aenean placerat. Ut imperdiet, enim sed gravida sollicitudin,
⁷ felis odio placerat quam, ac pulvinar elit purus eget enim. Nunc vitae tortor. Proin
⁸ tempus nibh sit amet nisl. Vivamus quis tortor vitae risus porta vehicula.

⁹ Fusce mauris. Vestibulum luctus nibh at lectus. Sed bibendum, nulla a faucibus
¹⁰ semper, leo velit ultricies tellus, ac venenatis arcu wisi vel nisl. Vestibulum diam.
¹¹ Aliquam pellentesque, augue quis sagittis posuere, turpis lacus congue quam,
¹² in hendrerit risus eros eget felis. Maecenas eget erat in sapien mattis porttitor.
¹³ Vestibulum porttitor. Nulla facilisi. Sed a turpis eu lacus commodo facilisis. Morbi
¹⁴ fringilla, wisi in dignissim interdum, justo lectus sagittis dui, et vehicula libero dui
¹⁵ cursus dui. Mauris tempor ligula sed lacus. Duis cursus enim ut augue. Cras ac
¹⁶ magna. Cras nulla. Nulla egestas. Curabitur a leo. Quisque egestas wisi eget nunc.
¹⁷ Nam feugiat lacus vel est. Curabitur consectetur.



2

1

Appendix

A Figures

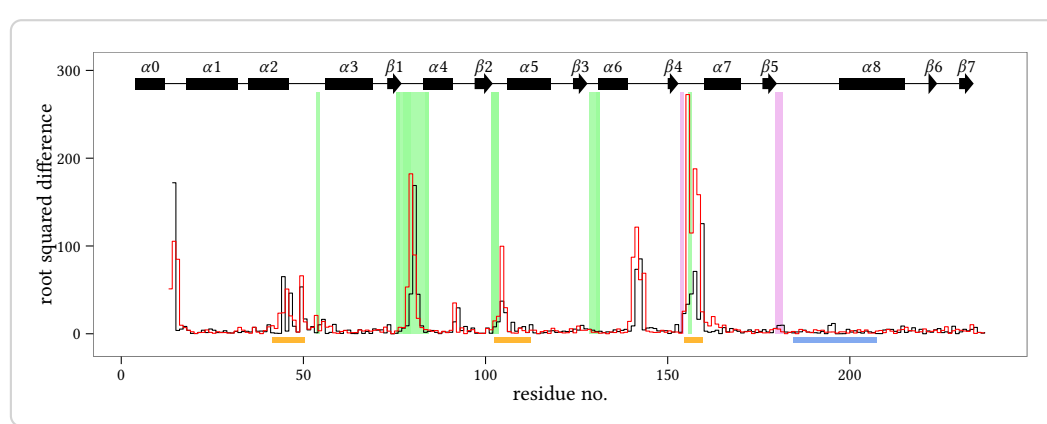


Figure A.1: Differences in the dihedrals ψ (red) and ϕ (black) of the solved apo-PFOMT and the structure with bound SAH (pdb: 3C3Y). The secondary structure is displayed at the top. Helices are displayed as rectangles and sheets are shown as arrows. Graphical background annotations are used to display the binding sites of SAH (green) and the metal ion (plum). The orange bars indicate regions, where much movement seems to happen upon binding or release of the co-substrate. The blue bar shows the region that was annotated as "insertion loop" in previous studies.

B Tables

Table B.3.: SAM analogues that have been used with MTs. Targets: P – peptide/protein, D – DNA, R – RNA, S – small molecule.

analogue	enzyme	target	references
<i>SAM</i>			
-CH ₂ -CH ₃	PRMT1, M.TaqI,	S,P,D	[114, 19, 108, 60] ¹
	M.HhaI, M.BcnIB, RebM, RapM		
-CH ₂ -CH ₂ -CH ₃	PRMT1, M.TaqI,	P,D	[114, 19]
	M.HhaI, M.BcnIB		
-CH ₂ -CH ₂ -CH ₂ -CH ₃	PRMT1	P	[114]
-CH ₂ -C ₆ H ₅	NovO, CouO,	S,P	[109, 114]
	PRMT1		
-CH ₂ -C(=O)-CH ₃	COMT, TPMT, CazF	S	[61, 125]

¹Singh *et al.* (2014) published a series of 44 biocatalytically synthesized SAM and SeAM derivatives, most of which were not tested towards their alkyl donation potential in MT reactions.

Appendix B. Tables

analogue	enzyme	target	references
$-\text{CH}_2-\text{CH}=\text{CH}_2$	NovO, CouO, RapM, PRMT1, M.TaqI, M.HhaI, M.BcnIB, RebM, Tgs	P,S,D	[109, 114, 19, 108, 121, 120, 113, 60, 101]
$-\text{CH}_2-\text{CH}=\text{CH}-\text{CH}_3$	NovO, CouO	S	[109]
$-\text{CH}_2-\text{C}\equiv\text{CH}$	Dim-5, HsMLL, TRM1, NovO, CouO, PRMT1	P,R,S	[123, 109, 121, 120, 48]
$-\text{CH}_2-\text{C}\equiv\text{N}$	RebM	S	[108]
$-\text{CH}_2-\text{CH}_2-\text{C}\equiv\text{CH}$	PKMT	P	[48]
$-\text{CH}_2-\text{CH}_2-\text{CH}_2-\text{C}\equiv\text{CH}$	PKMT	P	[48]
$-\text{CH}_2-\text{C}\equiv\text{C}-\text{CH}_3$	NovO, CouO, M.HhaI, M.TaqI, M.BcnIB	S,D	[109, 19, 70]
$-\text{CH}_2-\text{C}\equiv\text{C}-\text{CH}_2-\text{CH}_3$	M.HhaI	D	[70]
$-\text{CH}_2-\text{C}\equiv\text{C}-\text{CH}_2-\text{NH}_2$	M.HhaI	D	[70]
$-\text{CH}_2-\text{C}\equiv\text{C}-\text{CH}_2-\text{NH}-\text{C}(=\text{O})(-\text{CH}_2-)_3-\text{NH}_2$	M.HhaI	D	[70]
$-\text{CH}_2-\text{C}\equiv\text{C}(-\text{CH}_2-)_3-\text{NH}_2$	M.HhaI	D	[70]
$-\text{CH}_2-\text{C}\equiv\text{C}(-\text{CH}_2-)_3-\text{NH}-\text{C}(=\text{O})(-\text{CH}_2-)_3-\text{NH}_2$	M.HhaI	D	[70]
$-\text{CH}_2-\text{C}\equiv\text{C}(-\text{CH}_2-)_3-\text{C}\equiv\text{CH}$	M.HhaI	D	[70]
$-\text{CH}_2-\text{C}\equiv\text{C}(-\text{CH}_2-)_3-\text{N}_3$	M.HhaI	D	[70]
$-\text{CH}_2-\text{CH}=\text{CH}-\text{C}\equiv\text{CH}$	Dim-5, HsMLL, TRM1, PRMT1, Tgs	P,R	[123, 89, 121, 120, 82, 48, 101]
$-\text{CH}_2-\text{CH}=\text{CH}-\text{CH}_2-\text{C}\equiv\text{CH}$			[120, 48]

Appendix B. Tables

analogue	enzyme	target	references
$-\text{CH}_2-\text{CH}=\text{CH}-\text{CH}_2-\text{O}-\text{CH}_2-\text{C}\equiv\text{CH}$	PRMT1	P	[121, 120]
<i>SeAM</i>			
$-\text{CH}_3$			
$-\text{CH}_2-\text{C}\equiv\text{CH}$	Dim-5, <i>HsMLL</i> ,	P,R,S	[123, 108, 11, 125]
	TRM1, RebM, CazF		
<i>N</i> -mustard derivatives			
$-\text{CH}_2-\text{CH}_2-\text{I}$	RebM	S	[127]

Appendix B. Tables

Table B.1: Overview over the constructs produced for the present thesis. Each step during the production of the construct is given in the workflow steps column. Primers (*italic font*) or restriction sites used during each step are displayed in parenthesis.

construct name	description	entry constructs	destination	workflow steps (primers/cloning sites)
pBEW101	IsrA promoter	pBEW102	pBEW103	amplification (<i>pRha1.fw/rv</i>), cloning (BglII,
pBEW102	pBEW102 with BamHI cloning site	pBEW4b	BamHI)	
pBEW103	rhaP _{BAD} promoter			
pBEW104				
pBEW106	pICH413038-somt	pET28MC-somt	pICH413038	amplification (<i>smt1/2/3/4</i> , golden gate
				cloning (BpuI)
pBEW107			pICH75044	golden gate cloning (BsaI)
pBEW1a				
pBEW1b				
pBEW2a				
pBEW2b				
pBEW3a				
pBEW3b				
pBEW4a				
pBEW4b	<i>pfomt</i> gene in pET-28a(+), endogenous NdeI site removed	pQE30-pfomt	pET-28a(+)	mutagenesis (<i>pfo mt1.fw/rv</i>), amplification
pET28-pfomt				(<i>pfo mt2.fw/rv</i>), cloning (NdeI, EcoRI)
pET20-somt	N-terminal pelB-tag fusion for periplasmic expression		pET20-b(+)	
pET28-somt			pET28-a(+)	
pET28MC-somt				
pET32-somt				
pET741-somt	N-terminal TrX-tag fusion		pET-32a(+)	
pUC19*	N-terminal GST-tag fusion		pET-41a(+)	
pUCB1	added BglII site	pUC19	-	mutagenesis (<i>pUC1.fw/rv</i>)
pUCB1-sfGFP-DAS+4	pUCB1 derivative with IsrA promoter	lsr-XX-DAS	pUC19*	cloning (NdeI, BglII)

Appendix B. Tables

Table B.4: Crystallographic data, phasing and refinement statistics.

	140519_PFOMT	MC001413-G10.1
<i>data collection</i>		
wavelength (Å)		
resolution (Å)	1.95	
total reflections	392 368	
unique reflections	125 822	
completeness (%)	99.12	
$I/\sigma(I)$	9.9	
R_{sym}^a		
redundancy		
space group	$P2_12_12_1$	
cell dimensions (Å)		
<i>a</i>	86.16	48.88
<i>b</i>	128	71.36
<i>c</i>	129.3	127.80
<i>refinement</i>		
$R_{\text{work}}/R_{\text{free}}$	0.21369 / 0.24700	
rmsd bond lengths (Å)	0.0199	
rmsd bond angles (°)	2.0568	
B-values (Å ²)	21.593	
water		
ions		
<i>Ramachandran plot (%)</i>		
favoured	96.82	
allowed	2.38	
outliers	0.8	

C Affidavit

³ I hereby declare that this document has been written only by the undersigned and
⁴ without any assistance from third parties. Furthermore, I confirm that no sources
⁵ have been used in the preparation of this document other than those indicated in
⁶ the thesis itself.

¹ Date: , Location: , Signature:

²Bibliography

- 3 [1] Paul D. Adams et al. “PHENIX: A comprehensive Python-based system for
4 macromolecular structure solution”. en. In: *Acta Crystallographica Section*
5 *D: Biological Crystallography* 66.2 (Feb. 2010), pp. 213–221.
- 6 [2] Agilent Technologies. *QuikChange II Site-Directed Mutagenesis Kit: Instruction*
7 *Manual*. 2011.
- 8 [3] Neda Akbari et al. “Efficient refolding of recombinant lipase from Es-
9 cherichia coli inclusion bodies by response surface methodology.” In: *Protein*
10 *expression and purification* 70.2 (Apr. 2010), pp. 254–9.
- 11 [4] Martin Alexander and B. K. Lustigman. “Effect of Chemical Structure on
12 Microbial Degradation of Substituted Benzenes”. In: *Journal of Agricultural*
13 *and Food Chemistry* 14.4 (July 1966), pp. 410–413.
- 14 [5] Oyvind M. Andersen and Kenneth R. Markham, eds. *Flavonoids: Chemistry,*
15 *Biochemistry and Applications*. 1st ed. Boca Raton (FL): Taylor & Francis
16 Group, 2006.
- 17 [6] Bernd Anselment et al. “Experimental optimization of protein refolding
18 with a genetic algorithm”. In: *Protein Science* 19.11 (2010), pp. 2085–2095.
- 19 [7] Frederick M Ausubel et al. “Current Protocols in Molecular Biology”. In:
20 (2008), p. 23.
- 21 [8] Isabelle Benoit et al. “Expression in Escherichia coli, refolding and crys-
22 tallization of Aspergillus niger feruloyl esterase A using a serial factorial
23 approach.” In: *Protein expression and purification* 55.1 (Sept. 2007), pp. 166–
24 74.
- 25 [9] Olivier Binda et al. “A Chemical Method for Labeling Lysine Methyltrans-
1 ferase Substrates”. In: *ChemBioChem* 12.2 (2011), pp. 330–334.

Bibliography

Bibliography

- [10] Ian R Bothwell and Minkui Luo. "Large-scale, protection-free synthesis of Se-adenosyl-L-selenomethionine analogues and their application as cofactor surrogates of methyltransferases". In: *Organic Letters* 16.11 (2014), pp. 3056–3059.
- [11] Ian R. Bothwell et al. "Se-adenosyl-L-selenomethionine cofactor analogue as a reporter of protein methylation". In: *Journal of the American Chemical Society* 134.36 (2012), pp. 14905–14912.
- [12] George E. P. Box, J. Stuart Hunter, and William G. Hunter. *Statistics for Experimenters: Design, Innovation, and Discovery*. 2nd ed. New York: Wiley-Interscience, 2005.
- [13] Wolfgang Brandt, Kerstin Manke, and Thomas Vogt. "A catalytic triad – Lys-Asn-Asp – Is essential for the catalysis of the methyl transfer in plant cation-dependent O-methyltransferases". In: *Phytochemistry* 113 (2015), pp. 130–139.
- [14] Jhong-Min Chen et al. "Structural Insight into MtmC, a Bifunctional Ketoreductase-Methyltransferase Involved in the Assembly of the Mithramycin Trisaccharide Chain". In: *Biochemistry* 54.15 (2015), pp. 2481–2489.
- [15] Jih Jung Chen et al. "Dihydroagarofuranoid sesquiterpenes, a lignan derivative, a benzenoid, and antitubercular constituents from the stem of Microtropis japonica". In: *Journal of Natural Products* 71.6 (2008), pp. 1016–1021.
- [16] Vincent B Chen et al. "MolProbit: all-atom structure validation for macromolecular crystallography." In: *Acta crystallographica. Section D, Biological crystallography* 66.Pt 1 (Jan. 2010), pp. 12–21.
- [17] Al Claiborne and Irwin Fridovich. "Chemical and Enzymatic Intermediates in the Peroxidation of o-Dianisidine by Horseradish Peroxidase. 1. Spectral Properties of the Products of Dianisidine Oxidation". In: *Biochemistry* 18 (1979), pp. 2324–2329.
- [18] Yuntao Dai et al. "Natural deep eutectic solvents as new potential media for green technology." In: *Analytica chimica acta* 766 (Mar. 2013), pp. 61–8.
- [19] Christian Dalhoff et al. "Direct transfer of extended groups from synthetic cofactors by DNA methyltransferases." In: *Nature chemical biology* 2.1 (2006), pp. 31–32.
- [20] Christian Dalhoff et al. "Synthesis of S-adenosyl-L-methionine analogs and their use for sequence-specific transalkylation of DNA by methyltransferases." In: *Nature protocols* 1.4 (2006), pp. 1879–1886.

*Bibliography**Bibliography*

- 2 [21] Daresbury Laboratory. "No Title". In: *Newsletter on protein crystallography*
3 33 (1997), pp. 25–30.
- 4 [22] Martin Dippe, Lars Dressler, and Renate Ulbrich-Hofmann. "Fe(III)-
5 resorcylate as a spectrophotometric probe for phospholipid-cation interac-
6 tions." In: *Analytical biochemistry* 445 (Jan. 2014), pp. 54–9.
- 7 [23] Martin Dippe et al. "Engineering of a Mg²⁺-dependent O-methyltransferase
8 towards novel regiospecificity". In: *manuscript submitted* (2015).
- 9 [24] Martin Dippe et al. "Rationally engineered variants of S-adenosylmethionine
10 (SAM) synthase: reduced product inhibition and synthesis of artificial co-
11 factor homologues." en. In: *Chemical communications (Cambridge, England)*
12 51.17 (Feb. 2015), pp. 3637–40.
- 13 [25] J D Dunitz. "The entropic cost of bound water in crystals and biomolecules."
14 In: *Science (New York, N.Y.)* 264.5159 (Apr. 1994), p. 670.
- 15 [26] Jack D. Dunitz. "Win some, lose some: enthalpy-entropy compensation in
16 weak intermolecular interactions". In: *Chemistry & Biology* 2.11 (Nov. 1995),
17 pp. 709–712.
- 18 [27] Toru Egawa, Akiyo Kameyama, and Hiroshi Takeguchi. "Structural deter-
19 mination of vanillin, isovanillin and ethylvanillin by means of gas electron
20 diffraction and theoretical calculations". In: *Journal of Molecular Structure*
21 794 (2006), pp. 92–102.
- 22 [28] Elsevier. *Reaxys, version 2.19790.2*.
- 23 [29] P. Emsley et al. "Features and development of Coot". In: *Acta Crystallo-*
24 *graphica Section D: Biological Crystallography* 66.4 (2010), pp. 486–501.
- 25 [30] Carola Engler, Romy Kandzia, and Sylvestre Marillonnet. "A one pot, one
26 step, precision cloning method with high throughput capability". In: *PLoS*
27 *ONE* 3.11 (Jan. 2008), e3647.
- 28 [31] Philip Evans. "Scaling and assessment of data quality". In: *Acta Crystallo-*
29 *graphica Section D: Biological Crystallography* 62.1 (Jan. 2006), pp. 72–82.
30 arXiv: S0907444905036693 [doi: 10.1107].
- 31 [32] Matthew W Freyer and Edwin a Lewis. "Isothermal titration calorimetry:
32 experimental design, data analysis, and probing macromolecule/ligand bind-
33 ing and kinetic interactions." In: *Methods in cell biology* 84.07 (Jan. 2008),
34 pp. 79–113.
- 35 [33] Eva K Freyhult, Karl Andersson, and Mats G Gustafsson. "Structural model-
36 ing extends QSAR analysis of antibody-lysozyme interactions to 3D-QSAR."
1 In: *Biophysical journal* 84.4 (Apr. 2003), pp. 2264–72.

Bibliography

Bibliography

- 2 [34] Steffen Friedrich and Frank Hahn. "Opportunities for enzyme catalysis in
3 natural product chemistry". In: *Tetrahedron* 71.10 (2015), pp. 1473–1508.
- 4 [35] Rafael García-Meseguer et al. "Linking Electrostatic Effects and Protein
5 Motions in Enzymatic Catalysis. A Theoretical Analysis of Catechol O -
6 Methyltransferase". In: *The Journal of Physical Chemistry B* 119.3 (2015),
7 pp. 873–882.
- 8 [36] E. Gasteiger et al. "Protein Identification and Analysis Tools on the ExPASy
9 Server". In: *The Proteomics Protocols Handbook*. Ed. by John M. Walker.
10 Humana Press, 2005, pp. 571–607.
- 11 [37] S C Gill and P H von Hippel. "Calculation of protein extinction coefficients
12 from amino acid sequence data." In: *Analytical biochemistry* 182.2 (Nov.
13 1989), pp. 319–26.
- 14 [38] Paola Gilli et al. "Enthalpy-entropy compensation in drug-receptor binding".
15 In: *The Journal of Physical Chemistry* 98.5 (Feb. 1994), pp. 1515–1518.
- 16 [39] Markus Grammel and Howard C Hang. "Chemical reporters for biological
17 discovery." In: *Nature chemical biology* 9.8 (2013), pp. 475–84.
- 18 [40] Erich Grotewold, ed. *The Science of Flavonoids*. 1st ed. New York: Springer,
19 2006.
- 20 [41] Han Guo et al. "Profiling substrates of protein arginine N-methyltransferase
21 3 with S-adenosyl-L-methionine analogues". In: *ACS Chemical Biology* 9.2
22 (2014), pp. 476–484.
- 23 [42] Albert Hofmann. *Die Mutterkornalkaloide*. Solothurn: Nachtschatten Verlag,
24 2000.
- 25 [43] Scott Horowitz et al. "Conservation and functional importance of carbon-
26 oxygen hydrogen bonding in AdoMet-dependent methyltransferases". In:
27 *Journal of the American Chemical Society* 135.41 (2013), pp. 15536–15548.
- 28 [44] Ze Lin Huang et al. "Deep eutectic solvents can be viable enzyme activa-
29 tors and stabilizers". In: *Journal of Chemical Technology and Biotechnology*
30 October 2013 (2014).
- 31 [45] Ruth Huey et al. "A semiempirical free energy force field with charge-
32 based desolvation." In: *Journal of computational chemistry* 28.6 (Apr. 2007),
33 pp. 1145–52.
- 34 [46] Mwafaq Ibdah et al. "A Novel Mg²⁺-dependent O-Methyltransferase in the
35 Phenylpropanoid Metabolism of *Mesembryanthemum crystallinum*". In:
1 *Journal of Biological Chemistry* 278.45 (Nov. 2003), pp. 43961–43972.

*Bibliography**Bibliography*

- 2 [47] I Chemical Identity. "Chemical summary for vanillin". In: *Evaluation* 121
3 (1996), pp. 1–8.
- 4 [48] Kabirul Islam et al. "Expanding cofactor repertoire of protein lysine methyl-
5 transferase for substrate labeling". In: *ACS Chemical Biology* 6.7 (2011),
6 pp. 679–684.
- 7 [49] PD Josephy, T Eling, and RP Mason. "The horseradish peroxidase-catalyzed
8 oxidation of 3, 5, 3', 5'-tetramethylbenzidine. Free radical and charge-
9 transfer complex intermediates." In: *Journal of Biological Chemistry* 257
10 (1982), pp. 3669–3675.
- 11 [50] Wolfgang Kabsch. "Automatic processing of rotation diffraction data from
12 crystals of initially unknown symmetry land cell constants". In: *Journal of*
13 *Applied Crystallography* 26.pt 6 (Dec. 1993), pp. 795–800.
- 14 [51] Wolfgang Kabsch. "Integration, scaling, space-group assignment and post-
15 refinement". In: *Acta Crystallographica Section D: Biological Crystallogra-
16 phy* 66.2 (Feb. 2010), pp. 133–144.
- 17 [52] Wolfgang Kabsch. "Xds". In: *Acta Crystallographica Section D: Biological
18 Crystallography* 66.2 (Feb. 2010), pp. 125–132.
- 19 [53] K Kajiya et al. "Molecular bases of odor discrimination: Reconstitution of
20 olfactory receptors that recognize overlapping sets of odorants." In: *The
21 Journal of neuroscience : the official journal of the Society for Neuroscience*
22 21.16 (2001), pp. 6018–6025.
- 23 [54] Selin Kara et al. "Recent trends and novel concepts in cofactor-dependent
24 biotransformations". In: *Applied Microbiology and Biotechnology* 98.4 (2014),
25 pp. 1517–1529.
- 26 [55] Adler Kirk. "No Title". In: *Acta Chemica Scandinavica (1947-1973)* 24 (1970),
27 pp. 3379–3388.
- 28 [56] Youichi Kondou et al. "cDNA Libraries". In: *Methods in Molecular Biology*
29 729 (2011), pp. 183–197.
- 30 [57] Jakub G. Kopycki et al. "Biochemical and Structural Analysis of Substrate
31 Promiscuity in Plant Mg²⁺-Dependent O-Methyltransferases". In: *Journal
32 of Molecular Biology* 378.1 (Apr. 2008), pp. 154–164.
- 33 [58] Gerhard Krammer and Jenny Hartmann-Schreier. *Römpf Enzyklopädie On-
34 line*. 2015.
- 35 [59] Ulrich K Laemmli. "Cleavage of structural proteins during the assembly of
1 the head of bacteriophage T4." In: *Nature* 227.5259 (1970), pp. 680–685.

Bibliography

Bibliography

- 2 [60] Brian J. C. Law et al. “Site-specific bioalkylation of rapamycin by the RapM
3 16-O-methyltransferase”. In: *Chem. Sci.* (2015), pp. 2885–2892.
- 4 [61] Bobby W K Lee et al. “Enzyme-catalyzed transfer of a ketone group from
5 an S-adenosylmethionine analogue: A tool for the functional analysis of
6 methyltransferases”. In: *Journal of the American Chemical Society* 132.11
7 (2010), pp. 3642–3643.
- 8 [62] Jakob P. Ley et al. “Evaluation of bitter masking flavanones from Herba
9 Santa (*Eriodictyon californicum* (H. & A.) Torr., Hydrophyllaceae)”. In:
10 *Journal of Agricultural and Food Chemistry* 53.15 (2005), pp. 6061–6066.
- 11 [63] Jiaojie Li, Hua Wei, and Ming Ming Zhou. “Structure-guided design of a
12 methyl donor cofactor that controls a viral histone H3 lysine 27 methyltrans-
13 ferase activity”. In: *Journal of Medicinal Chemistry* 54.21 (2011), pp. 7734–
14 7738.
- 15 [64] Liwei Li et al. “PDBcal: a comprehensive dataset for receptor-ligand inter-
16 actions with three-dimensional structures and binding thermodynamics
17 from isothermal titration calorimetry.” In: *Chemical biology & drug design*
18 71.6 (June 2008), pp. 529–32.
- 19 [65] Zheng Li and Themis Lazaridis. “The effect of water displacement on binding
20 thermodynamics: Concanavalin A”. In: *Journal of Physical Chemistry B* 109.1
21 (2005), pp. 662–670.
- 22 [66] Zheng Li and Themis Lazaridis. “Water at biomolecular binding interfaces.”
23 In: *Physical chemistry chemical physics : PCCP* 9.5 (2007), pp. 573–581.
- 24 [67] Christopher A Lipinski. “Lead- and drug-like compounds: the rule-of-five
25 revolution.” In: *Drug discovery today. Technologies* 1.4 (Dec. 2004), pp. 337–
26 41.
- 27 [68] Christopher A Lipinski et al. “Experimental and computational approaches
28 to estimate solubility and permeability in drug discovery and develop-
29 ment settings1PII of original article: S0169-409X(96)00423-1. The article was
30 originally published in *Advanced Drug Delivery Reviews* 23 (1997) 3”. In:
31 *Advanced Drug Delivery Reviews* 46.1-3 (Mar. 2001), pp. 3–26.
- 32 [69] David K Liscombe, Gordon V Louie, and Joseph P Noel. “Architectures,
33 mechanisms and molecular evolution of natural product methyltrans-
34 ferases.” In: *Natural product reports* 29.10 (Oct. 2012), pp. 1238–50.
- 35 [70] Gražvydas Lukinavičius et al. “Enhanced chemical stability of AdoMet
36 analogues for improved methyltransferase-directed labeling of DNA”. In:
1 *ACS Chemical Biology* 8.6 (2013), pp. 1134–1139.

*Bibliography**Bibliography*

- 2 [71] Minkui Luo. "Current chemical biology approaches to interrogate protein
3 methyltransferases". In: *ACS Chemical Biology* 7.3 (2012), pp. 443–463.
- 4 [72] Tom J. Mabry, K. R. Markham, and M. B. Thomas. *The Systematic Identification
5 of Flavonoids*. Berlin, Heidelberg: Springer Berlin Heidelberg, 1970.
- 6 [73] Van Mai and Lindsay R Comstock. "Synthesis of an azide-bearing N-mustard
7 analogue of S-adenosyl-L-methionine". In: *Journal of Organic Chemistry*
8 76.24 (2011), pp. 10319–10324.
- 9 [74] Savvas C Makrides and Savvas C Makrides. "Strategies for Achieving High-
10 Level Expression of Genes in *Escherichia coli*". In: *Microbiological reviews*
11 60.3 (1996), pp. 512–538.
- 12 [75] S. V. Mani, D. W. Connell, and R. D. Braddock. "Structure activity relation-
13 ships for the prediction of biodegradability of environmental pollutants". en.
14 In: *Critical Reviews in Environmental Control* 21.3-4 (Jan. 1991), pp. 217–236.
- 15 [76] Kavitha Marapakala et al. "A disulfide-bond cascade mechanism for ar-
16 senic(III) <i>S</i>-adenosylmethionine methyltransferase". In: *Acta Crys-
17 tallographica Section D Biological Crystallography* 71.3 (2015), pp. 505–515.
- 18 [77] E. Neil G Marsh, Dustin P. Patterson, and Lei Li. "Adenosyl radical: Reagent
19 and catalyst in enzyme reactions". In: *ChemBioChem* 11.5 (2010), pp. 604–
20 621.
- 21 [78] Airlie J. McCoy. "Solving structures of protein complexes by molecular
22 replacement with Phaser". In: *Acta Crystallographica Section D: Biological
23 Crystallography* 63.1 (Jan. 2006), pp. 32–41.
- 24 [79] Airlie J. McCoy et al. "Phaser crystallographic software". In: *Journal of
25 Applied Crystallography* 40.4 (Aug. 2007), pp. 658–674.
- 26 [80] Edoardo Mentasti and Ezio Pelizzetti. "Reactions between iron(III) and
27 catechol (o-dihydroxybenzene). part I. Equilibria and kinetics of complex
28 formation in aqueous acid solution". en. In: *Journal of the Chemical Society,
29 Dalton Transactions* 23 (Jan. 1973), p. 2605.
- 30 [81] Garrett M Morris et al. "AutoDock4 and AutoDockTools4: Automated dock-
31 ing with selective receptor flexibility." In: *Journal of computational chem-
32 istry* 30.16 (Dec. 2009), pp. 2785–91.
- 33 [82] Yuri Motorin et al. "Expanding the chemical scope of RNA:methyltransferases
34 to site-specific alkynylation of RNA for click labeling". In: *Nucleic Acids
Research* 39.5 (2011), pp. 1943–1952.

Bibliography

Bibliography

- [83] Garib N. Murshudov, Alexei a. Vagin, and Eleanor J. Dodson. “Refinement of macromolecular structures by the maximum-likelihood method”. In: *Acta Crystallographica Section D: Biological Crystallography* 53.3 (May 1997), pp. 240–255.
- [84] Janet Newman. “Novel buffer systems for macromolecular crystallization”. In: *Acta Crystallographica Section D: Biological Crystallography* 60.3 (2004), pp. 610–612.
- [85] Siwen Niu et al. “Characterization of a sugar-O-methyltransferase TiaS5 affords new Tiacuminic analogues with improved antibacterial properties and reveals substrate promiscuity.” In: *Chembiochem : a European journal of chemical biology* 12.11 (July 2011), pp. 1740–8.
- [86] Novagen. *pET System Manual*. 11th ed. Darmstadt: EMD Chemicals, 2010.
- [87] Tanesha Osborne et al. “In situ generation of a bisubstrate analogue for protein arginine methyltransferase 1.” In: *Journal of the American Chemical Society* 130.14 (2008), pp. 4574–4575.
- [88] Ira Palmer and Paul T. Wingfield. “Preparation and extraction of insoluble (Inclusion-body) proteins from Escherichia coli”. In: *Current Protocols in Protein Science* 1.SUPPL.70 (Nov. 2012), Unit6.3.
- [89] Wibke Peters et al. “Enzymatic site-specific functionalization of protein methyltransferase substrates with alkynes for click labeling”. In: *Angewandte Chemie - International Edition* 49.30 (2010), pp. 5170–5173.
- [90] Harold R. Powell. “The Rossmann Fourier autoindexing algorithm in MOSFLM”. In: *Acta Crystallographica Section D: Biological Crystallography* 55.10 (1999), pp. 1690–1695.
- [91] R Core Team. *R: A Language and Environment for Statistical Computing*. Vienna, Austria, 2015.
- [92] Randy J. Read. “Pushing the boundaries of molecular replacement with maximum likelihood.” en. In: *Acta Crystallographica. Section D: Biological crystallography* 57.Pt 10 (Jan. 2001), pp. 1373–1382.
- [93] Michael Richter. “Functional diversity of organic molecule enzyme cofactors.” In: *Natural product reports* 30.10 (2013), pp. 1324–45.
- [94] M. G. Rossmann and D. M. Blow. “The detection of sub-units within the crystallographic asymmetric unit”. In: *Acta Crystallographica* 15.1 (Jan. 1962), pp. 24–31.

*Bibliography**Bibliography*

- 2 [95] Michael G. Rossmann. "Molecular replacement - Historical background". In:
3 *Acta Crystallographica - Section D Biological Crystallography* 57.10 (Sept.
4 2001), pp. 1360–1366.
- 5 [96] Rainer Rudolph and Hauke Lilie. "In vitro folding of inclusion body proteins".
6 In: *FASEB Journal* 10 (1996), pp. 49–56.
- 7 [97] Bernhard Rupp. *Biomolecular Crystallography: Principles, Practice, and Ap-*
8 *plication to Structural Biology*. 1st ed. New York: Garland Science, 2009,
9 p. 800.
- 10 [98] J H Ruth. "Odor thresholds and irritation levels of several chemical sub-
11 stances: a review." In: *American Industrial Hygiene Association journal* 47.3
12 (1986), A142–A151.
- 13 [99] J Sambrook and D W Russell. *Molecular Cloning: A Laboratory Manual*.
14 3rd ed. Cold Spring Harbor (NY, USA): Cold Spring Harbor Laboratory
15 Press, 2001.
- 16 [100] Cleydson Breno R Santos et al. "A SAR and QSAR study of new artemisinin
17 compounds with antimalarial activity". In: *Molecules* 19.1 (2014), pp. 367–
18 399.
- 19 [101] Daniela Schulz, Josephin Marie Holstein, and Andrea Rentmeister. "A
20 chemo-enzymatic approach for site-specific modification of the RNA cap".
21 In: *Angewandte Chemie - International Edition* 52.30 (2013), pp. 7874–7878.
- 22 [102] Daniela Schulz and Andrea Rentmeister. "Current Approaches for RNA
23 Labeling in Vitro and in Cells Based on Click Reactions". In: *ChemBioChem*
24 15.16 (2014), pp. 2342–2347.
- 25 [103] N. Schweigert, a. J B Zehnder, and R. I L Eggen. "Chemical properties of
26 catechols and their molecular modes of toxic action in cells, from microor-
27 ganisms to mammals". In: *Environmental Microbiology* 3.2 (2001), pp. 81–
28 91.
- 29 [104] Mark S. Searle, Martin S. Westwell, and Dudley H. Williams. "Application
30 of a generalised enthalpy?entropy relationship to binding co-operativity
31 and weak associations in solution". en. In: *Journal of the Chemical Society,*
32 *Perkin Transactions 2* 1 (Jan. 1995), p. 141.
- 33 [105] Stanley K. Shapiro and Dimis J. Ehninger. "Methods for the analysis and
34 preparation of adenosylmethionine and adenosylhomocysteine". In: *Ana-*
35 *lytical Biochemistry* 15.2 (May 1966), pp. 323–333.
- 36 [106] Alexander Shulgin and Ann Shulgin. *TiHKAL - The Continuation*. Ed. by
1 Dan Joy. 1st ed. Berkeley: Transform Press, 1997.

Bibliography

Bibliography

- [107] Sigma-Aldrich. *Technical Bulletin no. 2003-03: freezing of microbial samples prior to testing*. Parenteral Drug Association. 2003.
- [108] Shaneri Singh et al. "Facile chemoenzymatic strategies for the synthesis and utilization of S-adenosyl-L-methionine analogues". In: *Angewandte Chemie - International Edition* 53.15 (2014), pp. 3965–3969.
- [109] Harald Stecher et al. "Biocatalytic Friedel-Crafts alkylation using non-natural cofactors." In: *Angewandte Chemie (International ed. in English)* 48.50 (Jan. 2009), pp. 9546–8.
- [110] L. S. Stepanenko et al. "Characteristics of the far-eastern lichen Cetraria islandica". In: *Chemistry of Natural Products* 32.1 (1996), pp. 66–70.
- [111] Anna-Winona Struck et al. "S-Adenosyl-Methionine-Dependent Methyltransferases: Highly Versatile Enzymes in Biocatalysis, Biosynthesis and Other Biotechnological Applications." In: *Chembiochem : a European journal of chemical biology* (Nov. 2012), pp. 1–15.
- [112] F William Studier. "Protein production by auto-induction in high density shaking cultures." In: *Protein expression and purification* 41.1 (May 2005), pp. 207–234. arXiv: NIHMS150003.
- [113] Martin Tengg et al. "Molecular characterization of the C-methyltransferase NovO of Streptomyces sphaeroides, a valuable enzyme for performing Friedel–Crafts alkylation". In: *Journal of Molecular Catalysis B: Enzymatic* 84 (Dec. 2012), pp. 2–8.
- [114] Marie Thomsen et al. "Chemoenzymatic synthesis and in situ application of S-adenosyl-L-methionine analogs." In: *Organic & biomolecular chemistry* 11.43 (2013), pp. 7606–10.
- [115] Oleg Trott and Arthur J Olson. "AutoDock Vina: improving the speed and accuracy of docking with a new scoring function, efficient optimization, and multithreading." In: *Journal of computational chemistry* 31.2 (Jan. 2010), pp. 455–61.
- [116] Alexei a. Vagin et al. "REFMAC5 dictionary: Organization of prior chemical knowledge and guidelines for its use". en. In: *Acta Crystallographica Section D: Biological Crystallography* 60.12 I (Nov. 2004), pp. 2184–2195.
- [117] Thomas Vogt. "Regiospecificity and kinetic properties of a plant natural product O-methyltransferase are determined by its N-terminal domain". In: *FEBS Letters* 561.1-3 (Mar. 2004), pp. 159–162.

*Bibliography**Bibliography*

- 2 [118] Rui Wang and Minkui Luo. "A journey toward bioorthogonal profiling of
3 protein methylation inside living cells". In: *Current Opinion in Chemical*
4 *Biology* 17.5 (2013), pp. 729–737.
- 5 [119] Rui Wang, Weihong Zheng, and Minkui Luo. "A sensitive mass spectrum
6 assay to characterize engineered methionine adenosyltransferases with
7 S-alkyl methionine analogues as substrates". In: *Analytical Biochemistry*
8 450.1 (2014), pp. 11–19.
- 9 [120] Rui Wang et al. "Formulating a fluorogenic assay to evaluate S-adenosyl-L-
10 methionine analogues as protein methyltransferase cofactors". In: *Molecular*
11 *BioSystems* 7.11 (2011), p. 2970.
- 12 [121] Rui Wang et al. "Labeling substrates of protein arginine methyltransferase
13 with engineered enzymes and matched S-adenosyl-L-methionine analogues".
14 In: *Journal of the American Chemical Society* 133.20 (2011), pp. 7648–7651.
- 15 [122] Melissa Swope Willis et al. "Investigation of protein refolding using a frac-
16 tional factorial screen: a study of reagent effects and interactions." In: *Protein*
17 *Science* 14.7 (2005), pp. 1818–1826.
- 18 [123] Sophie Willnow et al. "A Selenium-Based Click AdoMet Analogue for Ver-
19 satile Substrate Labeling with Wild-Type Protein Methyltransferases". In:
20 *ChemBioChem* 13.8 (2012), pp. 1167–1173.
- 21 [124] Martyn D. Winn et al. "Overview of the CCP4 suite and current devel-
22 opments". In: *Acta Crystallographica Section D: Biological Crystallography*
23 67.4 (Apr. 2011), pp. 235–242.
- 24 [125] Jaclyn M. Winter et al. "Expanding the structural diversity of polyketides
25 by exploring the cofactor tolerance of an inline methyltransferase domain".
26 In: *Organic Letters* 15.14 (2013), pp. 3774–3777.
- 27 [126] Yingying Wu et al. "N-Methylation of the Amide Bond by Methyltrans-
28 ferase Asm10 in Ansamitocin Biosynthesis". In: *ChemBioChem* 12.11 (2011),
29 pp. 1759–1766.
- 30 [127] Changsheng Zhang et al. "Natural product diversification using a non-
31 natural cofactor analogue of S-adenosyl-L-methionine". In: *Journal of the*
32 *American Chemical Society* 128.9 (2006), pp. 2760–2761.
- 33 [128] Jun Zhang et al. "Arsenic Methylation and Volatilization by Arsenite
34 <i>S</i>-Adenosylmethionine Methyltransferase in *Pseudomonas al-*
35 *caligenes* NBRC14159". In: *Applied and Environmental Microbiology* 81.8
1 (2015), pp. 2852–2860.

² Acronyms

³ Å Ångström, 0.1 nm

⁴ **ABPP** activity based protein profiling 37

⁵ **AC-9** anthracene-9-carboxylic acid 23

⁶ **ATP** adenosine triphosphate 23

⁷ **BisTris** 2-[Bis(2-hydroxyethyl)amino]-2-(hydroxymethyl)propane-1,3-diol

⁸ **B-PER** bacterial protein extraction reagent

⁹ **CCP4** Collaborative Computational Project No. 4 26

¹⁰ **CD** circular dichroism 11

¹¹ **C-MT** C-methyl transferase 35

¹² **COMT** catechol O-methyl transferase 15

¹³ **Coot** Crystallographic Object-Oriented Toolkit 26

¹⁴ **CV** column volumes

¹⁵ **DMSO** dimethyl sulfoxide 25, 43

¹⁶ **DNA** desoxyribonucleic acid

¹⁷ **DNA MT** DNA methyl transferase vi, 35, 36

¹⁸ **DoE** design of experiments 21

¹⁹ **DTT** dithiothreitol; (2S,3S)-1,4-bis(sulfanyl)butane-2,3-diol

²⁰ **EDTA** ethylenediaminetetraacetic acid 17, 19–21, 30

²¹ **EEC** enthalpy-entropy compensation 39

²² **FFD** fractional factorial design ix, 21

¹ **FPLC** fast protein liquid chromatography 20, 32

*Acronyms**Acronyms*

- ² **FT** Fourier transformation 26
- ³ **GdmCl** guanidinium hydrochloride
- ⁴ **GFP** green fluorescent protein 27
- ⁵ **GOD** glucose oxidase 28
- ⁶ **GSH** glutathione, γ -L-glutamyl-L-cysteinylglycine 21, 28, 30
- ⁷ **GSSG** glutathione disulfide 21
- ⁸ **HEPES** 2-[4-(2-hydroxyethyl)piperazin-1-yl]ethanesulfonic acid
- ⁹ **HIC** hydrophobic interaction chromatography 32
- ¹⁰ **HPLC** high-performance liquid chromatography 14, 23, 30, 33
- ¹¹ **HRP** horseradish peroxidase 28
- ¹² **IB** inclusion body 19, 20, 22
- ¹³ **IEX** ion exchange chromatography 24
- ¹⁴ **IMAC** immobilized metal affinity chromatography
- ¹⁵ **IPB** Leibniz-Institute of Plant Biochemistry
- ¹⁶ **IPTG** isopropyl-D-thiogalactopyranosid 15, 18, 19
- ¹⁷ **ITC** Isothermal Titration Calorimetry vii, ix, 32, 33, 38, 39, 46
- ¹⁸ **LB** lysogeny broth 13, 15, 18, 19
- ¹⁹ **LC/MS** liquid chromatography coupled mass-spectrometry 41
- ²⁰ **MES** 2-(*N*-morpholino)ethanesulfonic acid
- ²¹ **MLU** Martin-Luther-Universität
- ²² **MMT** L-malic acid/MES/Tris 7, 33
- ²³ **MR** molecular replacement
- ²⁴ **MT** methyl transferase vi, ix, 34–37, 56
- ²⁵ **MTP** micro-titer plate 24, 25, 27, 28
- ²⁶ **MW** molecular weight 18
- ²⁷ **MWCO** molecular weight cut-off
- ²⁸ **NADES** natural deep eutectic solvent ix, 7, 25, 75
- ²⁹ **NPS** nitrogen, phosphate, sulfate buffer
- ¹ **NRPS** non-ribosomal peptide synthase 34
-

*Acronyms**Acronyms*

- ² **NTA** nitrilo triacetic acid 20
- ³ **O-MT** O-methyl transferase 28, 31, 33, 37
- ⁴ **PAGE** polyacrylamide gel electrophoresis 15–17, 22, 23, 32
- ⁵ **PBS** phosphate buffered saline 16, 22, 27
- ⁶ **PCH** propane-1,2-diol/choline chloride,NADES-mixture 25
- ⁷ **PCR** polymerase chain reaction 12
- ⁸ **PDA** photo diode array 33
- ⁹ **PDB** Protein Data Base 26, 27
- ¹⁰ **PFOMT** phenylpropanoid and flavonoid O-methyl transferase vii, 15, 18, 19, 24–28,
¹¹ 32, 33, 37–47
- ¹² **PHENIX** Phyton-based Hierarchical Environment for Integrated Xtallography 26
- ¹³ **PKS** poly ketide synthase 34
- ¹⁴ **PMSF** phenylmethylsulfonylfluoride
- ¹⁵ **P-MT** protein methyl transferase vi, 35, 36
- ¹⁶ **QSAR** quantitative structure activity relationship 34
- ¹⁷ **rmsd** root mean squared deviation 60
- ¹⁸ **rna** ribonucleic acid vi, 36
- ¹⁹ **RT** room temperature
- ²⁰ **SAE** S-adenosyl-L-ethionine, (2S)-2-amino-4-[[[(2S,3S,4R,5R)-5-(6-aminopurin-9-yl)-3,4-dihydroxyoxolan-2-yl]methyl-ethylsulfonio]butanoat vii, 23, 25, 35, 38–
²¹ 44, 47
- ²² **SAH** S-adenosyl-L-homocysteine vii, viii, 21, 30, 38–40, 42–47, 55
- ²³ **SAM** S-adenosyl-L-methionine vi, vii, ix, 23, 24, 28, 30, 35–42, 44, 46, 51, 56
- ²⁴ **SAMS** S-adenosylmethionine synthase 23
- ²⁵ **SAR** structure activity relationship 34
- ²⁶ **SDS** sodium dodecylsulfate 7, 15–17, 22, 23, 32
- ²⁷ **SeAM** Se-adenosyl selenomethionine vi, 35, 36, 56
- ²⁸ **SOMT-2** soy O-methyl transferase 15, 19, 21–23, 32
- ¹ **SSG** succinate/sodium phosphate/glycine 7

Acronyms

Acronyms

² **TB** terrific broth 15

³ **TCA** trichloro acetic acid 16, 17, 22, 30, 32

⁴ **Ti-plasmid** tumor inducing plasmid 9

⁵ **Tris** tris(hydroxymethyl)-aminomethane

⁶ **U** enzyme unit; measure for enzymatic activity (1 U = 1 µmole/min = 1/60 µkat)

⁷ **UV/VIS** ultra violet/visible (light spectrum) 24, 33

⁸ **V** volume

¹⁶⁰³ **ZYP** N-Z-amine, yeast extract, *p*hosphate 18

Glossary

¹⁶⁰⁴ **GOD** Glucose oxidase is an enzyme.... 74

¹⁶⁰⁵ **Isothermal Titration Calorimetry (ITC)** Fill in description here 74

¹⁶⁰⁷ **MTP** Micro-titer plate. Small format rectangular plastic plate containing wells
¹⁶⁰⁸ to allow for storage of multiple small samples or the containment multiple
¹⁶⁰⁹ simultaneous reactions. Typical sizes include 24, 96 and 384-wells 74

¹⁶¹⁰ **PFOMT** Phenylpropanoid and flavonoid O-methyl transferase from *Mesembryanthemum crystallinum*, which was first described by Ibdah et al. in 2003 [46]
¹⁶¹¹
¹⁶¹² 75

¹⁶¹³ **Ti-plasmid** Commonly found plasmids in *A. tumefaciens* and *A. rhizogenes* that
¹⁶¹⁴ confer virulence 76

¹⁶¹⁵ **ZYP-5052** Autoinduction medium developed by Studier [112]. The naming stems
¹⁶¹⁶ from the components N-Z-amine, yeast extract and phosphate. The numbering
¹⁶¹⁷ designates the composition; e.g. 5052 refers to 0.5 % glycerol, 0.05 % glucose and
¹⁶¹⁸ 0.2 % lactose. 76